

# Functional Profiling Identifies Genes Involved in Organ-Specific Branches of the PIF3 Regulatory Network in *Arabidopsis*

Maria Sentandreu,<sup>a</sup> Guiomar Martín,<sup>a</sup> Nahuel González-Schain,<sup>a</sup> Pablo Leivar,<sup>a</sup> Judit Soy,<sup>a</sup> James M. Tepperman,<sup>b,c</sup> Peter H. Quail,<sup>b,c</sup> and Elena Monte<sup>a,1</sup>

<sup>a</sup>Departament de Genètica Molecular, Center for Research in Agricultural Genomics, Centro Superior de Investigaciones Científicas-Institut de Recerca i Tecnologia Agroalimentàries-Universitat Autònoma de Barcelona-Universitat de Barcelona, Campus Universitat Autònoma de Barcelona, Bellaterra, 08193 Barcelona, Spain

<sup>b</sup>Department of Plant and Microbial Biology, University of California, Berkeley, California 94720

<sup>c</sup>United States Department of Agriculture, Plant Gene Expression Center, Albany, California 94710

**The phytochrome (phy)-interacting basic helix-loop-helix transcription factors (PIFs) constitutively sustain the etiolated state of dark-germinated seedlings by actively repressing deetiolation in darkness. This action is rapidly reversed upon light exposure by phy-induced proteolytic degradation of the PIFs. Here, we combined a microarray-based approach with a functional profiling strategy and identified four PIF3-regulated genes misexpressed in the dark (MIDAs) that are novel regulators of seedling deetiolation. We provide evidence that each one of these four MIDA genes regulates a specific facet of etiolation (hook maintenance, cotyledon appression, or hypocotyl elongation), indicating that there is branching in the signaling that PIF3 relays. Furthermore, combining inferred MIDA gene function from mutant analyses with their expression profiles in response to light-induced degradation of PIF3 provides evidence consistent with a model where the action of the PIF3/MIDA regulatory network enables an initial fast response to the light and subsequently prevents an overresponse to the initial light trigger, thus optimizing the seedling deetiolation process. Collectively, the data suggest that at least part of the phy/PIF system acts through these four MIDAs to initiate and optimize seedling deetiolation, and that this mechanism might allow the implementation of spatial (i.e., organ-specific) and temporal responses during the photomorphogenic program.**

## INTRODUCTION

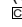
The phytochrome (phy) family of photoreceptors (phyA through phyE in *Arabidopsis thaliana*) plays a central role in the regulation of seedling deetiolation, the developmental transition from skotomorphogenesis to photomorphogenesis that dark-germinated seedlings undergo upon exposure to light (Rockwell et al., 2006; Schäfer and Nagy, 2006; Quail, 2010). After germination in the dark, etiolated seedlings grow heterotrophically on seed reserves and follow a skotomorphogenic strategy of development, characterized by fast hypocotyl elongation and maintenance of an apical hook and appressed cotyledons, to rapidly reach for sunlight at the soil surface. Upon reaching the surface, light triggers seedling deetiolation, the developmental switch to photomorphogenesis, which involves the coordinated inhibition of hypocotyl elongation, unfolding of the apical hook, separation and expansion of the cotyledons, and activation of functional

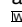
chloroplast and pigment biosynthesis to initiate photosynthesis. Photoactivation of the Pr form of the phy molecule during deetiolation results in rapid translocation of the Pfr form from the cytoplasm into the nucleus (Yamaguchi et al., 1999; Nagatani, 2004). Nuclear photoactivated phy molecules associate with phy-interacting factors (PIFs). The PIFs are a subset of basic helix-loop-helix transcription factors (PIF1, PIF3, PIF4, PIF5, PIF6, and PIF7 in *Arabidopsis*) that accumulate in the nucleus in the dark and interact conformer-specifically and photoreversibly with the phy-Pfr molecules in the light (Toledo-Ortiz et al., 2003; Duek and Fankhauser, 2005; Castillon et al., 2007; Monte et al., 2007). This phy-Pfr/PIF interaction initiates the gene expression changes that orchestrate the deetiolation response (Quail, 2002; Jiao et al., 2007; Bae and Choi, 2008). Nuclear interaction between active phyA and/or phyB and several of these transcription factors (including PIF1, PIF3, PIF4, and PIF5) has also been shown to induce rapid phosphorylation and degradation (within minutes) of the PIF proteins (Bauer et al., 2004; Park et al., 2004; Shen et al., 2005; Al-Sady et al., 2006; Oh et al., 2006; Nozue et al., 2007; Shen et al., 2007; Lorrain et al., 2008; Shen et al., 2008).

Recent studies with *Arabidopsis* seedlings deficient in one or multiple PIF proteins have established that progressive genetic removal of PIFs results in additive or synergistic effects in the dark that culminate in a partial *constitutively photomorphogenic (cop)*-like phenotype exhibited by the *pif* quadruple mutant *pif1*

<sup>1</sup> Address correspondence to elena.monte@cragenomica.es

The author responsible for distribution of materials integral to the findings presented in this article in accordance with the policy described in the Instructions for Authors (www.plantcell.org) is: Elena Monte (elena.monte@cragenomica.es).

 Some figures in this article are displayed in color online but in black and white in the print edition.

 Online version contains Web-only data.

www.plantcell.org/cgi/doi/10.1105/tpc.111.088161

*pif3 pif4 pif5 (pifq)*, which is deficient in PIF1, PIF3, PIF4, and PIF5 (Bae and Choi, 2008; Josse and Halliday, 2008; Leivar et al., 2008b). These results provide evidence that the PIF proteins function in the dark in a partially redundant manner, independently of phy action, to repress photomorphogenesis and promote skotomorphogenesis. Upon light exposure, active phy reverse this action by interacting with and inducing rapid degradation of the PIF proteins, allowing deetiolation to proceed.

The phy-mediated degradation of PIFs in dark-grown seedlings first exposed to light triggers the reduction of PIF protein levels to new steady state levels that represent ~10% of their dark levels (Monte et al., 2004; Shen et al., 2005; Nozue et al., 2007). *pif* mutant seedlings growing in continuous red light (Rc) display a hypersensitive phenotype that was initially interpreted as indicative of the PIFs having a negative role in phyB signaling in Rc (Huq and Quail, 2002; Kim et al., 2003; Fujimori et al., 2004; Monte et al., 2004; Khanna et al., 2007; de Lucas et al., 2008; Leivar et al., 2008a). However, more recent studies have shown that this phenotype is the result of elevated phyB levels in the absence of PIF proteins, an additive effect that correlates with increasing hypersensitivity to Rc with progressive genetic removal of multiple PIFs (Leivar et al., 2008a). Recently, Jang et al. (2010) have shown that the mechanism underlying the regulation of phyB levels (and other light-stable phys) during deetiolation involves direct interaction with the COP1 E3 ligase and that PIFs promote this interaction and the polyubiquitination of phyB by COP1.

Genome-wide expression analyses have started to provide some insight into the transcriptional network regulated by the PIFs. In dark-grown seedlings, transcriptomic profiling of single and double *pif1* (Moon et al., 2008), *pif3* (Leivar et al., 2009), and *pif4 pif5* (Lorrain et al., 2009) mutants have identified a small number of genes that are statistically and significantly deregulated in the mutants compared with their respective wild-type controls by at least twofold (Statistically Significantly and Two Fold [SSTF] genes). By contrast, microarray analysis of the *pifq* mutant compared with the wild type has resulted in the identification of a large subset of SSTF genes (~1000) that depend on PIF1, PIF3, PIF4, and PIF5 for their expression in the dark (Leivar et al., 2009; Shin et al., 2009). These results suggest redundancy at the molecular level between different members of the PIF family, similarly to their redundant contribution in establishing the *cop*-like visible phenotype of dark-grown *pifq* seedlings as explained above. The PIFq-regulated genes represent ~5% of the total genome and largely overlap with the transcriptome of wild-type seedlings grown under prolonged light, in accordance with the partial photomorphogenic phenotype of the *pifq* mutant in the dark (Leivar et al., 2009; Shin et al., 2009).

Some of these PIF-regulated genes are key regulators of pigment biosynthesis. PIF involvement in the regulation of chlorophyll biosynthesis became apparent upon transfer of 2-d-old or older dark-grown *pif* mutant seedlings to light, which failed to green (Huq et al., 2004; Stephenson et al., 2009). Microarray analysis identified the chlorophyll-biosynthesis-related genes *GLUTAMYL-tRNA REDUCTASE 1 (HEMA1)*, *Mg-CHELATASE H SUBUNIT (CHLH)*, *GENOMES UNCOUPLED 4 (GUN4)*, and *PROTOCHLOROPHYLLIDE OXIDOREDUCTASE C (PORC)* to present altered levels in *pif* mutants (Moon et al., 2008; Stephenson et al., 2009).

Misregulation of these genes in the dark results in exaggerated accumulation of the photooxidizing chlorophyll precursor protochlorophyllide in etiolated PIF-deficient seedlings, which causes photo bleaching upon transfer to light (Huq et al., 2004; Stephenson et al., 2009). PIFs also regulate the expression of the *PSY* gene encoding for the key carotenoid biosynthesis enzyme, which is upregulated during deetiolation to induce carotenoid accumulation (Toledo-Ortiz et al., 2010). In addition, many photosynthetic genes and genes associated with chloroplast biogenesis and function, like *LIGHT HARVESTING COMPLEX (LHC)* and *CHLOROPHYLL A/B BINDING PROTEIN (CAB)* genes, are also regulated by the PIFs in the dark (Moon et al., 2008; Leivar et al., 2009; Lorrain et al., 2009; Shin et al., 2009). This molecular phenotype is consistent with the partial conversion of etioplasts into chloroplasts exhibited by *pifq* seedlings in the dark (Leivar et al., 2009).

With the exception of pigment biosynthesis and chloroplast function, detailed analysis of the functional relevance of identified PIF-regulated genes in implementing the deetiolation program is still largely lacking (Leivar and Quail, 2011). Here, we identified an expanded set of genes that are regulated by PIF3 in the dark and examined their role in implementing seedling deetiolation by functional profiling of mutants. Integration of this information with the light-responsiveness of these genes is consistent with a model whereby the rapid initial deetiolation response is branched through PIF3-regulated genes and is subsequently counteracted to prevent an overresponse to light that could be detrimental for the emerging seedling.

## RESULTS

### PIF3 Represses Seedling Photomorphogenesis in the Dark by Regulating Gene Expression Both Positively and Negatively

Previous results have shown a role for PIF3 as negative regulator of photomorphogenesis in seedlings grown at specific time points in the dark (Leivar et al., 2008b; Stephenson et al., 2009). To characterize the role of PIF3 in more detail during extended periods of skotomorphogenic growth, we examined the morphological phenotype of the null *pif3-3* mutant (Monte et al., 2004) compared with the wild-type control during dark development for 4 d after germination (Figures 1A and 1B). During this period of dark growth, the wild-type hypocotyl elongates to ~12 mm, the hook partially and progressively unfolds to ~80°, and the cotyledons remain appressed. Compared with the wild type, *pif3* mutants are indistinguishable during germination and initial dark growth in the first 1.5 d (Figure 1A). By contrast, 2 d after germination, *pif3* mutants start displaying a partial photomorphogenic phenotype with more open hooks and cotyledons and marginal differences in hypocotyl elongation. These differences are maintained with increasing dark growth time up to 4 d of dark development (Figures 1A and 1B), in accordance with and expanding upon previous results by Leivar et al. (2008b) and Stephenson et al. (2009). Altogether, these results indicate that in the wild-type seedling growing in the dark for 4 d, cotyledons remain appressed, whereas there is a progressive elongation of the hypocotyl and

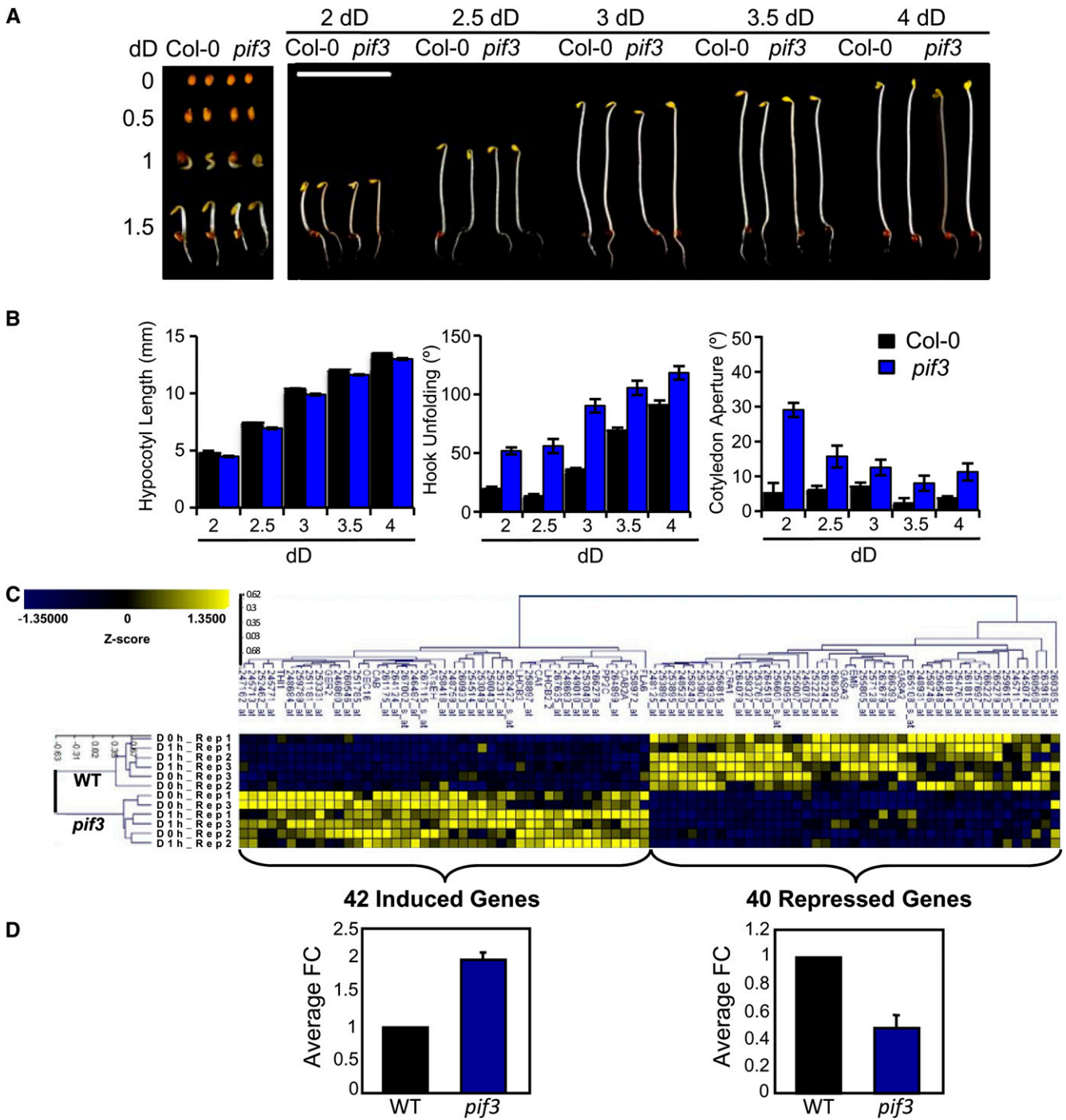


**Figure 1.** PIF3 Negatively Regulates Seedling Photomorphogenesis in the Dark from 2 d Onward after Germination.

**(A)** and **(B)** Characterization of the time of action of PIF3 during seedling etiolation in the dark. dD indicates days in the dark.

**(A)** Visual phenotype of representative seeds, embryos and seedlings for *Arabidopsis* wild-type Col-0 and *pif3-3* mutant seedlings in the dark at the indicated time points after germination.

**(B)** Quantification of hypocotyl length, hook unfolding, and cotyledon separation angle of *pif3-3* mutants compared with the wild-type Col-0 in the dark at the indicated time points after germination. Data represent the mean and SE of at least 30 seedlings.

**(C)** and **(D)** Regulation of gene expression in the dark by PIF3. Microarray expression profiling identified 82 HC target genes that are statistically significantly deregulated in the absence of PIF3 in the dark and by a FC greater than 1.5 (SS1.5F-HC).

**(C)** Two-dimensional-cluster diagram depicting the identified 82 SS1.5F-HC genes in 4-d-old dark-grown *pif3-3* seedlings compared with the wild-type

partial opening of the hook with increasing growth time in the dark. During this developmental process, PIF3 functions to repress photomorphogenesis from 2 d onward after germination and up to 4 d, with a role in promoting hypocotyl elongation and maintaining the hook and the cotyledons appressed, an effect that is sustained over time.

To identify downstream components that mediate PIF3 function as a repressor of photomorphogenesis in the dark, we first aimed to determine putative candidates by defining the PIF3-regulated transcriptome in the dark. To do so, we took advantage of a previous microarray study using Affymetrix ATH1 GeneChips, in which we analyzed the role of PIF3 in the regulation of phy-mediated gene expression in Rc (Monte et al., 2004). In that early work, our focus was to define the contribution of PIF3 in the regulation of the phy-mediated early transcriptional network in Rc. Here, given the current evidence that PIF3 and other PIF proteins act in the dark to sustain the skotomorphogenic state independently of phy activation (Bae and Choi, 2008; Leivar et al., 2008b), we analyzed the same raw microarray data (Monte et al., 2004), focusing now on the expression profiles in the dark (which were previously used exclusively to identify Rc responsive genes). In our current analysis, we took into consideration that, despite the obvious (although subtle) phenotypes observed for dark-grown *pif3* (Figures 1A and 1B) (Leivar et al., 2008b; Shin et al., 2009; Stephenson et al., 2009) and *pif1* (Leivar et al., 2008b; Shin et al., 2009; Stephenson et al., 2009) single mutant seedlings, previous microarray analysis of these mutants in the dark only identified 14 PIF3-regulated genes (Leivar et al., 2009) that were statistically and significantly expressed differently and by twofold (SSTF genes), and did not identify any SSTF genes regulated by PIF1 (Moon et al., 2008). Possible redundancy among PIFs in the regulation of gene expression (in accordance with their proposed redundant function as repressors of seedling deetiolation in the dark [Bae and Choi, 2008; Leivar et al., 2008b]) might translate into gene expression changes in single *pif* mutants smaller than SSTF. For this reason, we have decided to use a 1.5-fold cutoff in our new analysis presented here, a strategy that allowed Moon and colleagues to identify bona fide PIF1 targets (Moon et al., 2008).

Using the Rosetta Resolver platform (Rosetta Biosoftware), we analyzed two data sets of 4-d-old dark-grown seedlings (D0 h and D1 h) harvested 1 h apart and each including three biological replicates for wild type and three for *pif3-3* (Monte et al., 2004) (see Methods and Supplemental Figure 1A online). The complete analysis is presented in Supplemental Analysis 1 and associated Supplemental Figure 1 online; see also Supplemental References 1 online. This analysis identified a set of 121 PIF3-regulated genes (see Supplemental Figure 1A online) that are statistically and significantly expressed differently and by 1.5-fold in *pif3* compared

with the wild type (SS1.5F; see Supplemental Data Set 1 online), and a subset of 82 high-confidence (HC) PIF3 targets (SS1.5F-HC; see Supplemental Figure 1A and Supplemental Data Set 2 online). The gene list containing the 39 SS1.5F genes that did not make the HC cutoff is presented in Supplemental Data Set 3 online.

A two-dimensional cluster diagram representing the z-score-normalized signal intensities for the 82 SS1.5F-HC genes is shown in Figure 1C. The diagram contains the expression data for each of the six (three D0 h and three D1 h) wild-type and *pif3* biological replicates used in the analysis, and shows clustering of the 82 SS1.5F-HC genes in two subsets (induced and repressed) that have opposite expression patterns in their dependence on PIF3: approximately one-half of the 82 genes (40 genes) are repressed in *pif3* compared with the wild type, whereas the other one-half (42 genes) are induced (Figures 1C and 1D). The mean fold change (FC) for the up- and downregulated subset of genes is approximately twofold (Figure 1D). Further distribution of the 82 genes by FC is presented in Supplemental Analysis 1 and Supplemental Figure 1 online. It can be concluded that PIF3 represses photomorphogenesis in the dark, at least in part, by positively and negatively regulating the expression of the identified 40 and 42 genes, respectively (Figure 1D), and that, conversely, the misregulation of these genes in dark-grown *pif3* mutant seedlings might contribute to the observed phenotypes (Figures 1A and 1B). Functional classification of the 82 SS1.5F-HC genes is detailed in Supplemental Analysis 2 and the associated Supplemental Figure 2 online; see also Supplemental References 1 online. Notably, 25% of the annotated genes in the induced group in *pif3* relative to the wild type were photosynthesis-/chloroplast-related genes, indicating a degree of photomorphogenesis derepression in *pif3* consistent with its phenotype in the dark.

These expression patterns detected by microarray analysis were validated for selected genes by quantitative RT-PCR (qRT-PCR) analysis (see Supplemental Figure 3 online). Interestingly, the fold difference in expression between the wild type and the *pif3* mutant was more robust after 2 d of dark growth compared with 4 d for some of the tested genes (*AT5G16030*, *AT3G05730*, and *AT5G02760*) (see Supplemental Figure 3B online). These results suggest the existence of a developmentally regulated expression program during seedling growth in the dark. Similar observations were reported by Stephenson et al. (2009) for the behavior of three chlorophyll-biosynthesis genes (*HEMA1*, *GUN4*, and *CHLH*) in dark-grown *pif1*, *pif3*, and *pif1 pif3* mutants. In addition, seed batch variation could also account for some of the data variability, especially when differences are small, as previously reported (Leivar et al., 2008b).

To provide a broader molecular framework for the PIF3-regulated transcriptome in the dark defined here (Figures 1C and 1D; see Supplemental Figure 1 online), we compared it with

**Figure 1.** (continued).

(WT) Col-0. A total of 42 genes are upregulated (induced) in the absence of PIF3, whereas 40 correspond to genes that are downregulated (repressed), suggesting that PIF3 can act both as repressor and activator of gene expression in the dark.

**(D)** Mean FC for the 42 upregulated genes (left) and the 40 downregulated genes (right) in the *pif3-3* mutant in the dark relative to the wild-type dark value set at unity. Bars indicate SE for the genes averaged for each group.

Bar in **(A)** = 10 mm.

previous genome-wide studies on *pif4 pif5* (Lorrain et al., 2009) and *pifq* (Leivar et al., 2009). This comparative analysis is presented in Supplemental Analysis 3 online and is associated with Supplemental Figures 4 and 5 and Supplemental Data Set 4 online; see also Supplemental References 1 online. Consistent with the described phenotypic data (Leivar et al., 2008b, Shin et al., 2009; Stephenson et al., 2009), the comparative analysis suggests that PIF3 regulates gene expression in the dark in a partially redundant manner with other PIF factors, including PIF1, and that some specificity might exist among the genes targeted by PIF3 and PIF4/PIF5 in the presence of other PIFs.

### Selection of PIF3-Regulated *MISREGULATED IN DARK* Genes and Functional Characterization of *Arabidopsis mida* Mutants

The 82 PIF3-regulated genes identified by microarray analysis were considered good candidate genes to encode regulators of plant growth and development during the deetiolation process. To begin to determine whether some of them have functionally relevant roles in photomorphogenesis, we selected a subset of 10 genes functionally categorized as having potential transcription (*AT4G10240* and *AT5G04340*), signaling (*AT1G48260* and *AT5G02760*), growth and development (*AT4G37300*), stress and defense (*AT3G05730*), or hormone-related (*AT5G50600* and *AT4G10020*) activity, as well as two annotated as unknown (*AT3G47250* and *AT1G02470*), for systematic functional analysis using mutants. To this list, we have added three genes (*AT2G46070* encoding a MAPK kinase, and *AT1G05510* and *AT5G45690* of unknown function) from our SS1.5F gene set for their potential interest based on the predicted function (see Supplemental Analysis 2 online) and/or robust difference in expression in the *pifq* mutant (see Supplemental Analysis 3 online). Most of these genes show a response with respect to the wild type substantially more robust in the *pifq* mutant (Leivar et al. 2009) compared with *pif3* (see Supplemental Figure 6A online). Given that the two gene expression profile experiments were done using samples grown under different conditions (Monte et al., 2004; Leivar et al., 2009), we have validated these differences by qRT-PCR in *pif3* and *pifq* dark-grown seedlings grown at the same time and under the same conditions (see Supplemental Figure 6B online). These results suggest that these genes are targeted by PIF3 and possibly other PIFs during postgerminative growth in the dark.

These 13 genes were named *MISREGULATED IN DARK* (*MIDA*) genes. Table 1 contains a summary of these 13 *MIDA* genes, indicating for each one: *Arabidopsis* Gene Identification (AGI) number, previously ascribed name and reference (if published), FC in *pif3* with respect to the wild type, assigned functional group, our designated *MIDA* name, and the corresponding insertional mutant line isolated or the mutant line obtained if already available. The available mutants include one overexpressor line for *AT5G50600* (Li et al., 2007) and two RNA interference (RNAi) lines for *AT2G46070* (Lee et al., 2009). For *AT5G50600*, T-DNA insertional mutants were available; however, because the gene exists in two copies located in a large duplicated region, it is not possible to distinguish between homozygous and heterozygous lines, because the gene-specific

primers cross-hybridize with the intact copy of the duplicated gene (not carrying the T-DNA insertion) during the genotyping process, and thus prevent the identification of *AT5G50600* mutants that are suitable for characterization.

For the T-DNA insertional *mida* mutants, we identified homozygous mutant lines together with corresponding wild-type siblings for the phenotypic studies. For *mida6*, we were unable to find homozygous plants, even after analyzing the progeny of several heterozygous lines, indicating that the mutation might be lethal in homozygosity. All the *mida* mutant lines are in the ecotype Columbia (Col-0) background. Any phenotypes observed in the homozygous lines compared with their wild-type siblings were further confirmed by comparisons with Col-0 seedlings. The 12 mutated loci investigated over here were analyzed for statistically significant differences from the wild type in hypocotyl, cotyledon, and hook phenotypes in 2-, 3-, and 4-d-old dark-grown seedlings. Given the observed wild-type phenotypes during this period of dark development (Figures 1A and 1B), we reasoned that possible photomorphogenic phenotypes of the *mida* mutants might include deviations in both directions in hypocotyl growth (shorter or longer compared with the wild type) and/or in hook opening (decreased or increased angle with respect to the wild type), and deviations in cotyledon separation only in the direction of enhanced opening, because cotyledons remain essentially appressed in the wild type throughout dark development (Figures 1A and 1B). *mida* loss-of-function mutants showing a derepression of photomorphogenesis in the dark (i.e., displaying a shorter hypocotyl and/or a more open hook and cotyledons) would correspond to *MIDA* factors that potentially function as repressors of photomorphogenesis, whereas those showing enhanced skotomorphogenesis in the dark (i.e., displaying a longer hypocotyl and/or a closer hook) would correspond to *MIDA* factors with a potential role as inducers of photomorphogenesis.

Figure 2 and Supplemental Data Set 5 online show the functional characterization of *Arabidopsis mida* mutants in the dark, with the quantitative data and statistical analysis for hypocotyl length, hook unfolding, and cotyledon aperture. For comparison, data from multiple experiments are compiled in Figure 2, whereas the complete primary data and statistical analysis for each *mida* line are presented in Supplemental Data Set 5 online. For simplicity, data from each *mida* mutant line in Figure 2 are shown relative to their respective wild-type sibling set at unity, and a horizontal black dashed line set at 1 is included as the wild-type reference. An asterisk indicates the *mida* lines displaying statistically significant differences (see Methods) compared with their respective wild-type sibling in 2-, 3-, and 4-d-old dark-grown seedlings (see Supplemental Data Set 5 online for the associated P values). Even where statistically significant differences were detected (Figure 2; see Supplemental Data Set 5 online), the phenotypic differences between the wild type and *mida* lines ranged in magnitude from marginal to moderate. To define which lines display bona fide phenotypes, we applied a FC criterion, comparing the magnitude of the phenotype to their respective wild-type sibling (Figure 2; see Supplemental Data Set 5 online). Based on the phenotypes displayed by single and double PIF-deficient mutants (Leivar et al., 2008b), we set a FC cutoff at 40% for the hook, 80% for the cotyledon, and 20% for

**Table 1.** List of the 13 *MIDA* Genes Analyzed, Including the AGI Loci, the Designated Protein Names, the FC in Expression in *piF3* Mutant in the Dark Relative to the Wild Type, and Their Functional Category

<i>MIDA</i>	AGI No.	Protein Name	FC at D0 h <i>piF3</i> versus Wild Type	Functional Category	Reported Function	Mutant Line	<i>Mida Line</i>
<i>MIDA1</i>	AT5G50600	HSD1	-1.61226	H	Li et al. (2007)	AOHSD16 (Li et al., 2007)	<i>mida1-OX</i>
<i>MIDA2</i>	AT3G05730	DEFL	2.78217	S/D	ND	SALK_031670	<i>mida2</i>
<i>MIDA3</i>	AT4G37300	MEE59	1.54716	G/D	ND	SALK_040468	<i>mida3</i>
<i>MIDA4</i>	AT1G02470	UNKNOWN	2.33482	UNK	ND	SALK_123221	<i>mida4</i>
<i>MIDA5</i>	AT3G47250	UNKNOWN	1.568	UNK	ND	SALK_099356	<i>mida5</i>
<i>MIDA6</i>	AT5G04340	ZN FINGER	-2.04231	TXN	ND	SALK_140448	<i>mida6</i>
<i>MIDA7</i>	AT1G48260	CIPK17	-1.76389	S	ND	SALK_130764	<i>mida7</i>
<i>MIDA8</i>	AT4G10020	HSD5	-1.50981	H	ND	SAIL_129B11	<i>mida8</i>
<i>MIDA9</i>	AT5G02760	PP2C	1.76423	S	ND	SAIL_764H11	<i>mida9-1</i>
<i>MIDA9</i>	AT5G02760	PP2C	1.76423	S	ND	SALK_672093	<i>mida9-2</i>
<i>MIDA10</i>	AT4G10240	BBX23	-1.50432	TXN	ND	SALK_053389C	<i>mida10</i>
<i>MIDA11</i>	AT2G46070	MPK12	1.679	S	Lee et al. (2009)	MPK12RNAi-9 (Lee et al., 2009)	<i>mida11-1</i>
<i>MIDA11</i>	AT2G46070	MPK12	1.679	S	Lee et al. (2009)	MPK12RNAi-17 (Lee et al., 2009)	<i>mida11-2</i>
<i>MIDA12</i>	AT1G05510	UNKNOWN	-2.5	UNK	ND	SALK_117754	<i>mida12</i>
<i>MIDA13</i>	AT5G45690	UNKNOWN	-1.705	UNK	ND	SALK_145109	<i>mida13</i>

The corresponding mutant lines isolated from SALK or SAIL, and the previously identified mutants are indicated together with their *mida* nomenclature. Functional categories: G/D, growth/development; H, hormone; S, signaling; S/D, stress/defense; TXN, transcription; UNK, unknown. ND, not determined.

the hypocotyl (represented by horizontal red dashed dotted lines in Figure 2). In addition, given the variation in gene expression during dark development (see Supplemental Figures 3 and 4E online), which suggests that the action of PIF3-regulated genes might have variable relevance during the process of skotomorphogenesis, we required that the statistically significant differences and FC cutoffs had to be met in at least 2 d. Together, based on these three defined criteria (P value, FC, and time of action), mutations in four genes caused apparent photomorphogenic seedling phenotypes in the dark (Figure 2): *mida9* and *mida10* showed enhanced hook unfolding, whereas *mida11* displayed shorter hypocotyls, and *mida1-OX* had more separated cotyledons. These results suggest branching of the signal that PIF3 relays through the MIDAs to regulate specific aspects of the deetiolation response. Figures 3 and 4 show a more detailed characterization of these *mida* mutants (see below).

### MIDA9 and MIDA10 Are Novel Repressors of Hook Unfolding

Figure 3 shows the *mida9* and *mida10* phenotypes, together with a more detailed characterization of the *mida* mutants, a diagram of the *MIDA* gene that indicates the position of the T-DNA insertion, and an RNA gel blot that confirms the disruption of the transcript in the *mida* mutant. A bar graph showing the FC difference in expression in the *piF3* mutant compared with the wild type in the dark is also included.

For *MIDA9*, a PIF3-repressed gene (Figure 3C), we identified a T-DNA insertional allele, designated *mida9-1*, that carries a T-DNA insertion in the first exon, from the Syngenta Arabidopsis Insertion Library (SAIL) collection (Figure 3A, Table 1). The *mida9-1* allele produced no detectable *MIDA9* transcript and is therefore likely a null (Figure 3B). Hook unfolding phenotypes of two mutant siblings compared with a wild-type sibling and with Col-0 showed that the

*mida9* mutant exhibited enhanced hook unfolding after 2, 3, and 4 d in the dark (Figures 3D and 3E). Similar results were obtained for a second null mutant allele of *MIDA9* (*mida9-2*) (Table 1; see Supplemental Figure 7 online). *MIDA9* encodes a previously uncharacterized type 2C phosphatase, predicted to be nuclear, belonging to the D clade of type 2C phosphatases in *Arabidopsis* (Schweighofer et al., 2004). Based on these results, we conclude that *MIDA9* is a PIF3-repressed repressor of photomorphogenesis in the dark with a specific role in hook unfolding.

For *MIDA10*, a PIF3-induced gene (Figure 3H), we identified a T-DNA insertional allele designated *mida10-1* from the SALK collection (Alonso et al., 2003; <http://signal.salk.edu>) that carries a T-DNA insertion in the second exon (Figure 3F, Table 1). The *mida10-1* allele produced no detectable *MIDA10* transcript and is therefore likely a null (Figure 3G). Hook unfolding phenotypes of a wild-type sibling and two mutant siblings compared with Col-0 show the enhanced hook unfolding of the *mida10* mutant after 3 and 4 d in the dark (Figures 3I and 3J). *MIDA10* encodes B-BOX CONTAINING PROTEIN 23 (BBX23) (Datta et al., 2008; Khanna et al., 2009). *BBX23/MIDA10* belongs to a clade among the B-Box family of proteins that consists of eight genes, with several of its related members previously implicated in light-dependent development (Datta et al., 2008 and references therein; Khanna et al., 2009). Based on these results, we conclude that *BBX23/MIDA10* is a PIF3-induced repressor of photomorphogenesis in the dark with a specific role in hook unfolding. For simplicity, we refer to *BBX23/MIDA10* as *MIDA10* hereafter.

### MIDA11 Is a Novel Regulator of Hypocotyl Elongation

*mida11* is a previously published dexamethasone (DEX)-inducible RNAi line (Table 1) (Lee et al., 2009). It was originally shown to have a phenotype in root elongation under continuous

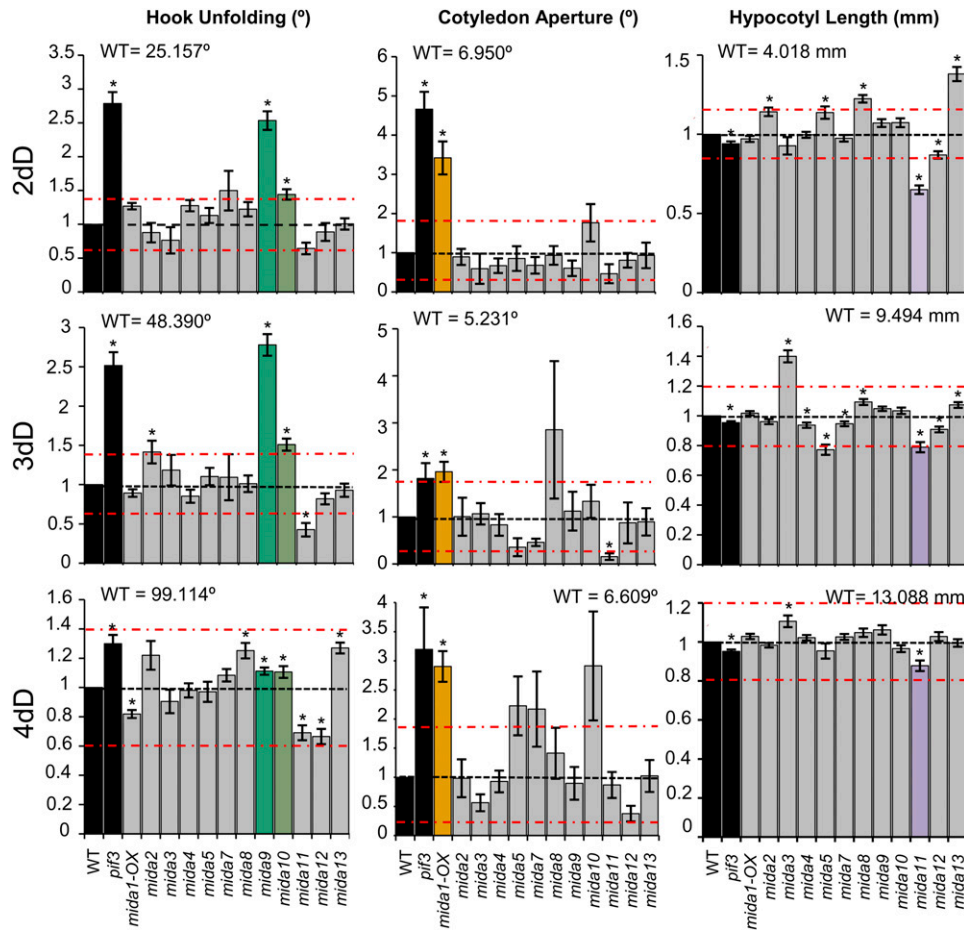


**Figure 2.** Functional Characterization of *Arabidopsis mida* Mutants Defective in PIF3 Target Genes Identifies Four Novel Regulators of Seedling Deetiolation.

Hook unfolding angle (left), cotyledon separation angle (middle), and hypocotyl length (right), displayed by 2- (top), 3- (middle), and 4-d-old (bottom) *mida* mutant lines. A total of 30 seedlings were used for measurements, and values were normalized to the corresponding wild-type (WT) sibling (see Supplemental Data Set 5 online for primary data and statistical analysis). For each *mida* line, a corresponding wild-type sibling was used as control to calculate the P value and FC difference (see Methods and Supplemental Data Set 5 online for further details). In the bar graph, measurements for *mida* mutant lines are expressed as a FC with respect to their wild-type sibling, whereas error bars represent the variation (SE) of this FC response of at least 30 seedlings (see Supplemental Data Set 5 online). For comparison purposes, a wild type set at unity is shown as reference (shown as horizontal dashed line). The *pif3* mutant is also included as reference. Based on statistical difference (P value < 0.05) (marked with an asterisk in the graph) together with a FC relative to the corresponding wild type greater than 40% for hook, and/or 80% for cotyledon, and/or 20% for hypocotyl (these cutoff percentage values are indicated by a dashed dotted line) in at least two of the 3 d assayed, four *mida* lines were determined to display a partial photomorphogenic phenotype in the dark: *mida9* and *mida10* display partially open hooks, *mida11* displays short hypocotyls, and *mida1-OX* displays partially separated cotyledons. The actual degrees of aperture or the length of the hypocotyl of an average wild-type response from the multiple experiments is indicated as reference on the top of each graph (see Supplemental Data Set 5 online for the calculation). The *mida9* and *mida11* mutant alleles used were *mida9-1* and *mida11-2*, respectively. [See online article for color version of this figure.]

white light (WLC) (Lee et al., 2009). Figure 4B shows the effect of DEX on the amount of *MIDA11* transcript in the wild type and two independent *mida11* (*mida11-1* and *mida11-2*) dark-grown seedlings, indicating that *mida11* has reduced levels in the dark (a 60 to 80% reduction compared with the wild type) in the presence of DEX. DEX application induced a hypocotyl phenotype in both *mida11* RNAi lines compared with the control Col-0 treated with DEX (Figures 4C and 4D). *MIDA11*, a PIF3-repressed gene (Figure 4A), encodes a MAP kinase (MPK12) that has been proposed to regulate auxin signaling (Lee et al., 2009).

Based on these results, we conclude that MPK12/MIDA11 is a PIF3-repressed repressor of photomorphogenesis in the dark with a specific role in hypocotyl elongation. For simplicity, we refer to MPK12/MIDA11 as MIDA11 hereafter.

#### MIDA1 Is a Novel Regulator of Cotyledon Separation

*mida1-OX* is a previously published *HYDROXYSTEROID DEHYDROGENASE 1 (HSD1)* overexpressor line (Table 1) (Li et al., 2007). It was originally shown to exhibit a growth phenotype in

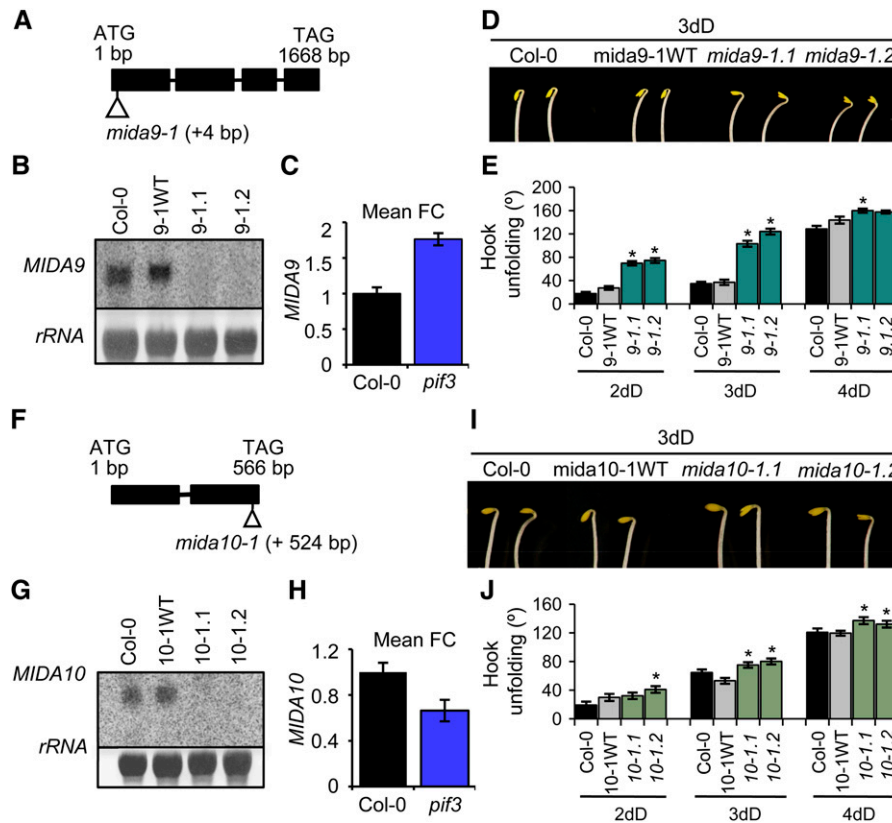


**Figure 3.** MIDA9 and MIDA10 Are Novel Repressors of Hook Unfolding in the Dark.

(A) The mutation identified in *Arabidopsis MIDA9*. The T-DNA insert in *mida9-1* is indicated at position +4 bp relative to the ATG.  
 (B) RNA gel blots of 2-d-old, dark-grown Col-0, *mida9-1.1*, and *mida9-1.2* mutant seedlings, and a corresponding *mida9-1* wild-type (WT) sibling. No *MIDA9* transcript was detected in *mida9-1*, indicating that it is likely a functional knockout mutant.  
 (C) Bar graph of microarray data showing the FC in *MIDA9* expression in *pif3* relative to the wild-type in the dark. Data correspond to biological triplicates, and bars indicate SE.  
 (D) Visual hook phenotype of 3-d-old, dark-grown Col-0, wild-type sibling, and *mida9-1* mutant seedlings.  
 (E) Quantification of hook angle in *mida9-1* compared with Col-0 and a wild-type sibling line after 2, 3, and 4 d of growth in the dark (dD) after germination. Data represent the mean and SE of at least 30 seedlings, and asterisks indicate statistically different mean values compared with their corresponding wild type.  
 (F) The mutation identified in *Arabidopsis MIDA10*. The T-DNA insert in *mida10-1* is indicated at position +524 bp relative to the ATG.  
 (G) RNA gel blot of 2-d-old, dark-grown Col-0, *mida10-1.1*, and *mida10-1.2* mutant seedlings, and a corresponding *mida10-1* wild-type sibling. No *MIDA10* transcript was detected in *mida10-1*, indicating that it is likely a functional knockout mutant.  
 (H) Bar graph of microarray data showing the FC in *MIDA10* expression in *pif3* relative to the wild type in the dark. Data correspond to biological triplicates and bars indicate SE.  
 (I) Visual hook phenotype of 3-d-old dark-grown Col-0, a wild-type sibling, and *mida10-1* seedlings.  
 (J) Quantification of hook angle in *mida10* compared with Col-0 and a wild-type sibling line after 2, 3, and 4 d of growth in the dark after germination. Data represent the mean and SE of at least 30 seedlings, and asterisks indicate statistically different mean values compared with their corresponding wild type. [See online article for color version of this figure.]

adult plants grown in WLC conditions (Li et al., 2007). Figure 4F shows the expression levels of *HSD1/MIDA1* in two overexpressor lines grown in the dark, indicating that *mida1-OX* exhibits increased levels of *HSD1/MIDA1* in the dark (between 1.5-fold to fourfold compared with the wild type). Enhanced cotyledon separation in these two overexpressor lines compared with Col-0 after 2, 3, and 4 d in the dark is shown in Figures 4G and 4H. *HSD1/MIDA1*, a PIF3-induced gene (Figure 4E), has been proposed to encode an enzyme involved in brassinosteroid (BR) synthesis (Li et al., 2007). Based on these results, we conclude

that *HSD1/MIDA1* is a PIF3-induced inducer of photomorphogenesis in the dark with a specific role in cotyledon separation. For simplicity, we refer to *HSD1/MIDA1* as *MIDA1* hereafter.

#### Light-Responsiveness of PIF3-Regulated Genes in the Dark

The above data are summarized in Supplemental Table 1 online and suggest that PIF3 action in the dark involves the induction of *MIDA10* and *MIDA1*, a negative and a positive regulator of photomorphogenesis, respectively, and the repression of *MIDA9*



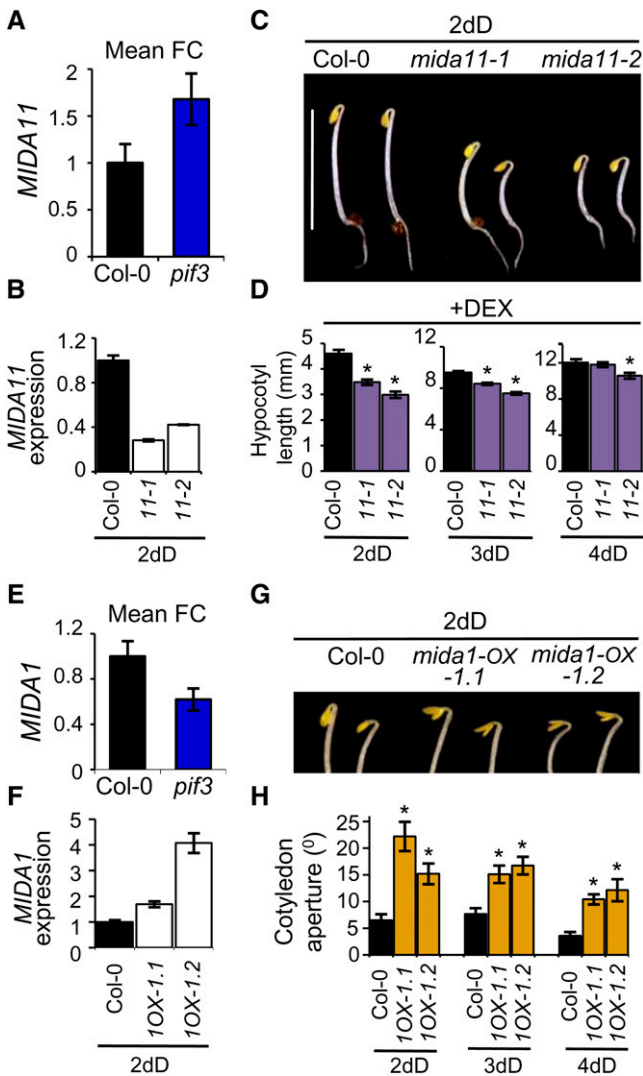


**Figure 4.** *MIDA11* Is a Novel Inducer of Hypocotyl Length and *MIDA1* Is a Novel Regulator of Cotyledon Separation in the Dark.

**(A)** Bar graph of microarray data showing the FC in *MIDA11* expression in *pif3* relative to the wild type in the dark. Data correspond to biological triplicates, and bars indicate SE.

**(B)** qRT-PCR analysis of 2-d-old, dark-grown Col-0 and *mida11-1* and *mida11-2* mutant seedlings grown in the presence of DEX. Expression levels were normalized to *PP2A* as described previously (Shin et al., 2007) and expressed relative to the wild-type value set at unity. *MIDA11* transcript levels were reduced ~80% in the two lines used, confirming that *MIDA11* expression is suppressed by the DEX-induced RNAi in dark conditions. *mida11-1* and *mida11-2*, two independent RNAi lines, were obtained from Lee et al. (2009) (Table 1). Error bars represent SE values of technical triplicates.

**(C)** Visual hypocotyl phenotype of 3-d-old dark-grown Col-0 and *mida11-1* and *mida11-2* seedlings in the presence of DEX.

**(D)** Quantification of hypocotyl length in *mida11* compared with Col-0 after 2, 3, and 4 d of growth in the dark (dD) after germination in the presence of DEX. Data represent the mean and SE of at least 30 seedlings, and asterisks indicate statistically different mean values compared with their corresponding wild type.

and *MIDA11*, both negative regulators of photomorphogenesis in the dark (Figures 2 to 4). These data provide a complex and somewhat contradictory picture of how PIF3 might exert its function as a repressor of photomorphogenesis. To further analyze how this complex regulatory network might participate during seedling deetiolation, we next addressed the question of how the rapid phy-induced degradation of PIF3 (and other PIFs) upon illumination of dark-grown seedlings might affect the expression of the four identified *MIDAs*.

To do this, we reanalyzed the light data from the same microarray experiment (wild type after 1 h of Rc [R1 h], included in Monte et al., 2004, and the previously unpublished wild type [E. Monte and P. Quail, unpublished data] after 18 h of Rc [R18 h]), using the Rosetta Resolver software for consistency (see Methods). We defined early (R1 h) and late (R18 h) red light-responsive genes as genes that display SSTF alterations when comparing the wild type after 1 h of Rc (R1 h) versus the wild type kept in darkness for 1 h (D1 h) and the wild type after 18 h of Rc (R18 h) versus the wild type kept in darkness for 18 h (D18 h), respectively. We identified 546 R1 h SSTF genes and 2764 R18 h SSTF genes in our experiment. Supplemental Data Sets 6 and 7 online show the gene lists containing R1 h SSTF and R18 h SSTF genes, respectively. We then compared the genes displaying SS1.5F-HC alterations in *pif3* after 4 d in darkness (*pif3*-D) with genes displaying SSTF alterations in the wild type after R1 h and after R18 h. This comparative analysis is presented in Supplemental Analysis 4, the associated Supplemental Figure 8, and Supplemental Data Set 8 online; see also Supplemental References 1 online. Notably, 67% of *pif3*-D genes were light-responsive at R1 h and/or R18 h, with 83.6% of these responding to Rc later than 1 h after illumination (see Supplemental Figure 8A and Supplemental Analysis 4 online).

To establish the light-responsive kinetics of the four *MIDA* genes identified to have a role in deetiolation (Figures 3 and 4), we combined the R1 h and R18 h microarray information for each gene (see Supplemental Figure 9 online) with a detailed time-

**(E)** Bar graph of microarray data showing the fold change in *MIDA1* expression in *pif3* relative to the wild type in the dark. Data correspond to biological triplicates and bars indicate SE.

**(F)** qRT-PCR analysis of 2-d-old, dark-grown wild type and *mida1-OX* mutant seedlings. Expression levels were normalized to *PP2A* as described previously (Shin et al., 2007) and expressed relative to the wild-type value set at unity. *MIDA1* transcript was overexpressed in *mida1-OX-1.1* and *mida1-OX-1.2*, confirming that the lines overexpress *MIDA1* in dark conditions. Overexpressor *mida1-OX-1.1* and *mida1-OX-1.2* lines (represented in the figure as 1OX-1.1 and 1OX-1.2, respectively) are two siblings from a transgenic line obtained from Li et al. (2007) (Table 1). Error bars represent SE values of technical triplicates.

**(G)** Visual cotyledon phenotype of 2-d-old, dark-grown Col-0 and *mida1-OX-1* seedlings.

**(H)** Quantification of cotyledon angle in *mida1-OX-1* (represented as 1OX-1 in the figure) compared with Col-0 after 2, 3, and 4 d of growth in the dark after germination. Data represent the mean and SE of at least 30 seedlings, and asterisks indicate statistically different mean values compared with their corresponding wild type.

Bar in **(C)** = 5 mm.

[See online article for color version of this figure.]

course qRT-PCR analysis of 2-d-old dark-grown wild-type seedlings exposed to Rc for increasing periods of time (Figure 5A). Our results show that light triggers an immediate early response of the *MIDA10* transcript, with a 10-fold light repression at 1 h compared with dark levels, and reaches almost nondetectable levels after 12 h of Rc exposure (Figure 5A). *MIDA1* also responds early with a sixfold induction after 2 h of Rc exposure in 2-d-old dark-grown seedlings (Figure 5A). This induction of *MIDA1* in light conditions is transient, and transcript levels return to dark levels after 6 h of irradiation (Figure 5A). Finally, Rc triggers a twofold induction of *MIDA9* and *MIDA11* transcripts relative to their dark control after 3 and 6 to 9 h, respectively (Figure 5A), an induction that decreases again after 18 h of Rc (see Supplemental Figure 9 online). For all four genes, expression levels in the *pif3* mutant kept in the dark during this time showed little variation (Figure 5A). These qRT-PCR results validate and expand on the microarray data at R1 h and R18 h for these genes (see Supplemental Figure 9 online), and together indicate that the rapid phy-induced degradation of PIF3 triggers a light response in all four *MIDA* genes in the wild type that is in the same direction as the alteration in expression caused by PIF3 deficiency in the dark: One is light-repressed (*MIDA10*), and three are light-induced (*MIDA9*, *MIDA11* and *MIDA1*). In addition, these results indicate that PIF3 degradation triggers an early light response in *MIDA10* and *MIDA1* and a late light response in *MIDA9* and *MIDA11* (Figure 5A). Altogether, these data suggest that the *MIDA* factors induced by light (*MIDA9*, *MIDA11*, and *MIDA1*) might not only

have a role during skotomorphogenesis in the dark but also function during deetiolation either early (after 1 to 3 h of Rc) and/or late (after more than 3 h of Rc) once the seedling has been exposed to light.

### Participation of the MIDAs in the Seedling Responses to Light

We examined the phenotypes of *mida9*, *mida10*, *mida11*, and *mida1-OX* in the dark-to-Rc transition. Figure 5B shows the results for each of the mutants. For *mida10*, 2-d-old etiolated seedlings show a weak unfolded hook phenotype in the dark (Figures 2, 3J, and 5B), and exposure to light accelerates the hook opening response compared with the corresponding wild type, resulting in an aperture of 40° after 3 h (Figure 5B). These results suggest that *MIDA10* acts as a repressor of hook opening during the initial deetiolation response, consistent with its role as a hook repressor in the dark (Figures 2, 3I, and 3J) and its rapid degradation upon exposure to light (Figure 5A). For *mida1-OX*, the differences in cotyledon separation between the mutant and the wild type in the dark (Figures 2, 4G, 4H, and 5B) are larger in response to Rc (Figure 5B): Cotyledons in 2-d-old wild-type seedlings are basically appressed in the dark (10° aperture) and start responding to light 12 h after Rc exposure, to reach an aperture of 80° after 24 h of illumination. By contrast, the cotyledons of *mida1-OX* are partially separated in the dark (30°, threefold the wild-type aperture), start responding to Rc

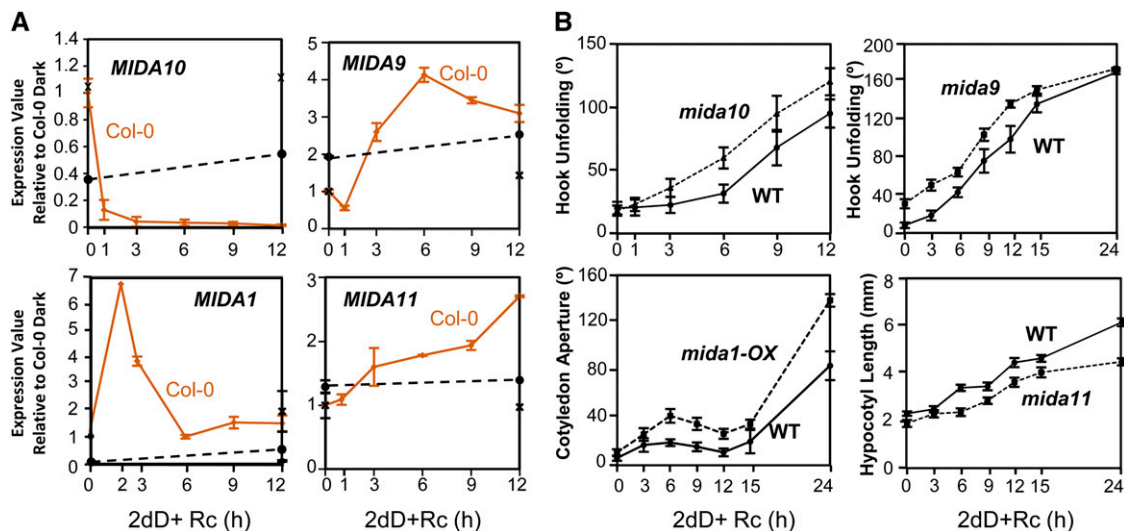


**Figure 5.** Light-Responsiveness of *MIDA* Gene Expression and Phenotypic Characterization of *mida* Mutants during the Dark-to-Light Transition.

**(A)** Light-responsiveness of selected PIF3-regulated *MIDA* genes in dark-grown wild-type (WT) seedlings exposed to Rc (8  $\mu\text{mol}/\text{m}^2/\text{s}$ ). Wild-type siblings were exposed to Rc for increasing periods from 0 (dark control) to 12 h, and expression levels were assayed by qRT-PCR, normalized to *PP2A* as described previously (Shin et al., 2007), and expressed relative to the Col-0 dark value set at unity. Expression levels in the *pif3* mutant in the dark are indicated with a dashed line for comparison. The expression level in Col-0 maintained in the dark for 12 h is indicated in the graph with an X. Error bars correspond to SE values of technical triplicates.

**(B)** Time-course quantification of hook opening (*mida9* and *mida10*), cotyledon separation (*mida1-OX*), and hypocotyl growth (*mida11*) (in the presence of DEX), of 2-d-old, dark-grown wild type (WT) (solid lines) and *mida* mutant seedlings (dashed lines) during the dark-to-red light transition. Data represent the mean and SE of at least 30 seedlings.

[See online article for color version of this figure.]

earlier than the wild type (after only 3 h of illumination), and reach an angle of 140° after 24 h of Rc. These results indicate that MIDA1 functions as an inducer of cotyledon separation during early deetiolation, consistent with the observed phenotype of *mida1-OX* in the dark (Figures 2, 4G, and 4H) and with the rapid MIDA1 induction in response to Rc (Figure 5A). For *mida9*, our results showed more open hooks in *mida9* mutants compared with the wild type over the time-course analysis in response to light (Figure 5B). This effect is difficult to attribute specifically to light, given that *mida9* hooks are already opened in the dark (Figures 2, 3D, 3E, and 5B), similar to the hook response of *pif* mutants in the dark and in the dark-to-light response (Leivar et al., 2008b). Alternative evidence of a role for MIDA9 in hook repression in the light was obtained by growing seedlings continuously in low far-red light (FR) (see Supplemental Figure 10 online). In these conditions, the wild-type hooks are only partially opened after 4 d (aperture of 120°), and the hooks of *mida9* seedlings are wider open (160°) (see Supplemental Figure 10 online). These data suggest a role for MIDA9 as a repressor of hook unfolding in the dark (Figures 2, 3D, and 3E) and in the light, consistent with the observed phenotype of *mida9* in the dark (Figures 2, 3D, and 3E) and with the MIDA9 induction in response to light (Figure 5A). Finally, for the DEX-inducible *mida11*, the differences in hypocotyl length between the mutant and the wild type in the dark (Figures 2, 4C, and 4D) increase in response to Rc in the presence of DEX (Figure 5B). Whereas the wild-type seedlings grow from 2.4 mm in the dark to 6.2 mm after 24 h of Rc, *mida11* seedlings grow from 1.9 mm in the dark (20% shorter than the wild type) to only 4.4 mm after 24 h of Rc (30% shorter than the wild type at the same time point) (Figure 5B). Hypocotyl elongation rate in *mida11* compared with the wild type seems to be progressively affected over time after the first 3 h of light exposure (Figure 5B). As a control, etiolated *mida11* seedlings grown in the absence of DEX showed no difference in hypocotyl length in the dark or in the transition to light compared with the control (see Supplemental Figure 11 online). These results indicate that MIDA11 functions as a repressor of hypocotyl elongation inhibition in the dark-to-light transition (Figure 5B), with a more prominent role after 3 h of light exposure, consistent with the observed phenotype of *mida11* in the dark (Figures 2, 4C, and 4D) and with the induction of MIDA11 in response to Rc (Figure 5A).

Altogether, our data suggest that the apparent contradiction of having PIF3 in the dark induce MIDA10 and MIDA1, a negative and a positive regulator of photomorphogenesis, respectively, and repress MIDA9 and MIDA11, both negative regulators, can be explained if one considers the early or late light responsiveness of these MIDA factors as well as their time of action in the dark-to-light transition. A summary of the above data regarding light responsiveness of the four MIDA genes and light phenotypes of their *mida* mutants, integrated with the results of our previous analysis of the expression of each gene in seedlings grown in the dark, is shown in Supplemental Table 1 online. For MIDA10, these data suggest a simple scenario, where early PIF3/phy-mediated light repression allows the rapid removal of a dark hook repressor, which facilitates the rapid hook unfolding that occurs during the initiation of deetiolation. Likewise, for MIDA1, the early PIF3/phy-mediated induction upon exposure of the

seedling to light allows for the rapid accumulation of a cotyledon separation inducer, which contributes to cotyledon separation during the initiation of deetiolation. Given that *mida1-OX* is an overexpressor mutant line (Figure 4F), the high levels of MIDA1 in this mutant in the dark compared with those of the wild type possibly mimic the levels reached in the wild type after light induction, and *mida1-OX* mutant seedlings display a phenotype of separated cotyledons in the absence of light. Also, the transient nature of its light induction suggests that after a few hours of illumination, the expression of MIDA1 is repressed to stop its cotyledon separation action. MIDA10 and MIDA1 might therefore participate in the dark and/or the early (1 to 3 h of Rc) steps of deetiolation induction of hook unfolding and cotyledon separation. By contrast, MIDA9 and MIDA11 are both repressors of photomorphogenesis (specifically of hook opening and of the inhibition of hypocotyl elongation, respectively) that are late light-induced (after 3 to 6 h of Rc) and seem to function not only in the dark but also during deetiolation, once the seedling has been exposed to light (Figure 5B).

Interestingly, our unexpected finding that the seedlings possess photomorphogenesis repressors (MIDA9 and MIDA11) that are late light-induced (after 3 to 6 h of Rc), is consistent with the existence of a PIF3/phy-mediated regulatory response in the deetiolation process that might function after deetiolation is initiated. This late (after 3 to 6 h of Rc) regulatory response could represent a mechanism for the seedling to moderate the rapid initial response.

### PIF3 Together with Other PIFs Prevent an Exaggerated Inhibition of Hypocotyl Elongation and Cotyledon Separation in Response to Light

PIFs have been previously reported to be negative regulators of hypocotyl elongation in Rc conditions, with PIF-deficient mutants showing hypersensitivity to Rc (Huq and Quail, 2002; Kim et al., 2003; Fujimori et al., 2004; Monte et al., 2004; Khanna et al., 2007; de Lucas et al., 2008; Leivar et al., 2008a). However, a possible role for the PIFs in the regulation of hypocotyl inhibition in the initial dark-to-light transition has not been explored. We examined the inhibition of hypocotyl elongation in *pif3* and *pif3 pif4 pif5* mutants. Figure 6A shows that dark-grown wild-type seedlings respond to the light trigger by inhibiting hypocotyl elongation and reducing the hypocotyl growth rate. Red light has been shown to induce inhibition of hypocotyl growth in dark-grown seedlings exposed to Rc during the first 3 h of illumination, effectively slowing down the hypocotyl growth rate (Parks and Spalding, 1999). This inhibition begins to decrease after 3 h of irradiation, and seedlings in red light keep growing at a reduced speed compared with seedlings maintained in darkness (Parks and Spalding, 1999). In accordance, our results show that the wild-type hypocotyls elongate from 3.8 mm to 8 mm 24 h after exposure to Rc, whereas seedlings kept in the dark maintain a more constant hypocotyl growth speed and reach 9.6 mm (Figure 6A). Strikingly, *pif3 pif4 pif5* seedlings almost completely stop elongating after exposure to light (Figure 6A). This phenotype suggests that there is an exaggerated inhibition of hypocotyl elongation during deetiolation in the absence of PIF3, PIF4, and PIF5. *pif3 pif4 pif5* mutants maintained in the dark during this

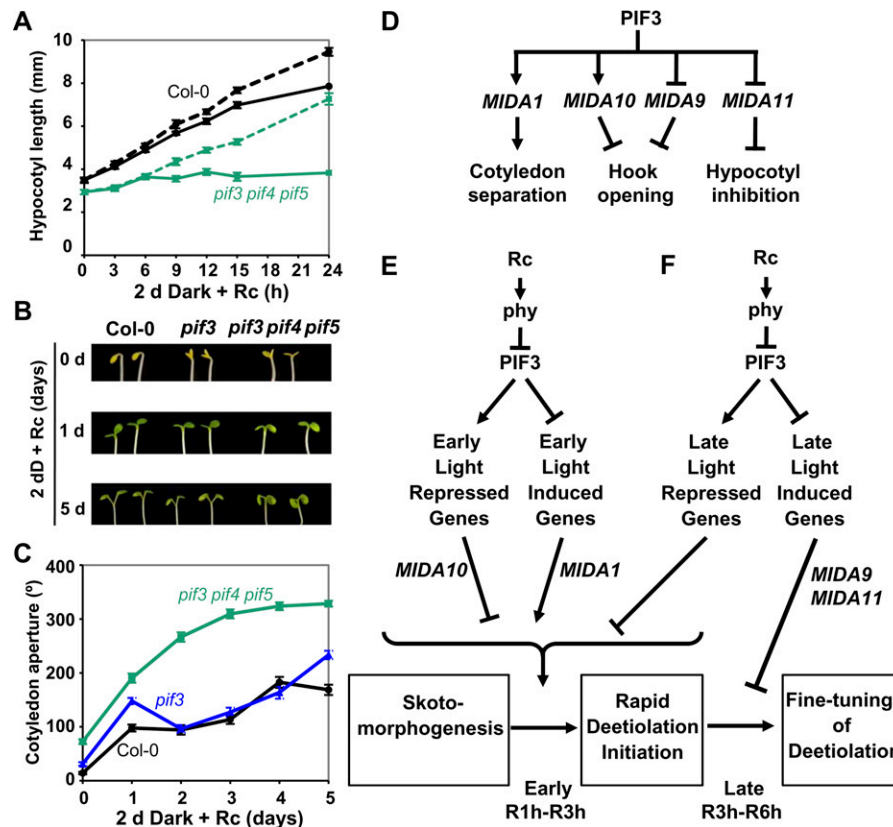


**Figure 6.** PIF-Regulated Transcriptional Network.

(A) to (C) Dark-grown PIF-deficient seedlings exhibit an exaggerated response to Rc ( $8 \mu\text{mol}/\text{m}^2/\text{s}$ ).

(A) Time-course quantification of hypocotyl length of 2-d-old dark-grown Col-0 and *pif3 pif4 pif5* seedlings kept in the dark (dashed lines) or during the dark-to-light transition (solid lines) for 24 h. Data represent the mean and SE of at least 30 seedlings.

(B) Visual phenotype of 2-d-old, dark-grown Col-0, *pif3*, and *pif3 pif4 pif5* seedlings exposed to 0, 1, or 5 d of Rc.

(C) Time-course quantification of cotyledon separation of 2-d-old, dark-grown Col-0, *pif3*, and *pif3 pif4 pif5* seedlings during the transition to Rc light for 5 d. Data represent the mean and SE of at least 30 seedlings.

(D) Simplified schematic model depicting the branching in the signaling that PIF3 relays to regulate specific aspects of deetiolation, like cotyledon separation, hook opening, and hypocotyl inhibition through the MIDAs.

(E) and (F) Simplified schematic model depicting the PIF3-dependent *MIDA* transcriptional network that regulates seedling deetiolation in response to phy-mediated light signals. PIF3 acts constitutively in darkness as either a transcriptional repressor or activator, resulting in the regulation of *MIDA* gene expression. Phy-mediated, light-induced degradation of PIF3 triggers reversal of PIF3 action on *MIDA* genes that are early (E) or late (F) light-responsive. Early (1 h) light-responsive genes rapidly initiate deetiolation in response to phy-mediated PIF degradation (E), acting either as light-induced inducers (such as *MIDA1*) or light-repressed repressors (such as *MIDA10*) of deetiolation. By contrast, late (3 to 6 h) light-responsive genes (F) have the opposite function to slow down and fine-tune the initial response and optimize seedling deetiolation, as exemplified here by *MIDA9* and *MIDA11*.

period kept growing at the same rate (Figure 6A). Single *pif3* mutants exhibit only a marginal phenotype after exposure to Rc (see Supplemental Figure 12A online), suggesting that PIF3 might be redundant to other PIFs, including PIF4 and PIF5, in the regulation of hypocotyl elongation during the dark-to-light transition, as has previously been described for skotomorphogenesis in the dark (Bae and Choi, 2008; Leivar et al., 2008b).

PIF-deficient mutants have also been shown to have more separated cotyledons during the dark-to-light transition, a phenotype that is partially established in the dark, and reach a maximum angle of  $180^\circ$  during the first 24 h of illumination (Leivar et al., 2008b). Closer examination of *pif3 pif4 pif5* mutant seedlings during extended Rc exposure after 2 d of dark growth

reveals a striking cotyledon overseparation in response to light. The cotyledons of the wild-type seedlings separate to  $\sim 100^\circ$  after 24 h of exposure to Rc (Figures 6B and 6C). This fast response is followed by a slower response over the next 3 d of growth in Rc, when cotyledons reach a maximum angle of  $185^\circ$  (i.e., perpendicular to the hypocotyl), effectively maintaining an optimum angle for light perception (Figures 6B and 6C). The cotyledons of the wild-type seedlings kept in darkness for this time period remain appressed (see Supplemental Figure 12B online). Compared with the wild-type seedlings, *pif3 pif4 pif5* mutants exhibit partially separated cotyledons in the dark ( $60^\circ$ ), as previously described (Leivar et al., 2008b), and have a fast initial response during the first 24 h of light exposure that is similar

in magnitude to the wild-type response, reaching a cotyledon separation of 200° (Figures 6B and 6C). However, in contrast with the wild type, this fast response is maintained over the next 3 d of growth in Rc to reach a cotyledon separation of 310° (Figures 6B and 6C). The cotyledons of *pif3 pif4 pif5* mutants maintained in the dark during this time period open from 60° to 150° (see Supplemental Figure 12B online), a difference that was greatly amplified by light (Figures 6B and 6C). The response of *pif3* (which reaches a cotyledon angle of 240°) is also greater than the wild-type response (which reaches 185° of cotyledon aperture, as detailed above) (Figures 6B and 6C). These results indicate that, in the absence of PIF3, seedlings undergo exaggerated cotyledon separation in response to light, suggesting that PIF3 regulates the inhibition of cotyledon separation. A detailed examination of *pif3 pif4 pif5* also shows an overresponse during the first 24 h of exposure to light (see Supplemental Figure 12C online), as occurs to a lesser extent in *pif3* (see Supplemental Figure 12C online) (Leivar et al., 2008b). Together, our data indicate that the PIF proteins have an important role in preventing the overseparation of cotyledons during seedling establishment, with PIF3 acting in a partially redundant manner to PIF4 and PIF5.

## DISCUSSION

Despite much progress in recent years, our understanding of how PIFs function during seedling deetiolation is incomplete, partly because the role of PIF target genes remains largely unknown. In this study, we have expanded on the morphological and molecular characterization of the *pif3* mutant to identify bona fide target genes of PIF3 action in the dark. Functional profiling of the identified PIF3-target genes suggests branching of the signaling that PIF3 relays to regulate specific facets of deetiolation, such as hypocotyl elongation, cotyledon separation, and hook opening. The regulation of these downstream organ-specific targets by light is consistent with a model of PIF3/MIDA action that enables an initial fast response to the light and subsequently prevents overresponses to the light trigger.

### Branching of PIF3 Signaling through Four Novel PIF3-Regulated MIDA Factors to Regulate Different Facets of Seedling Development in the Dark

Our analysis of PIF3-regulated gene expression in etiolated seedlings shows that, in darkness, PIF3 regulates 82 genes (Figure 1; see Supplemental Figure 1 online). With the objective of determining to what extent these PIF3-regulated genes are necessary for transducing the PIF3 signal during seedling deetiolation, we selected 13 PIF3 target genes (*MIDA1* to *MIDA13*) based on their predicted function for systematic analysis of mutant phenotypes (Table 1). Our phenotypic data analysis determined that four of the *MIDA* genes mutagenized in this study (*MIDA9*, *MIDA10*, *MIDA11*, and *MIDA1*) exhibit significant perturbation of the etiolated phenotypes and represent novel regulators of seedling development in the dark (Figure 2). Expression analyses by qRT-PCR and microarray suggest that these *MIDA* factors are likely targeted by other PIFs in addition to PIF3 (see Supplemental Figure 6 and Sup-

plemental Analysis 3 online), because their response is more robust in *pifq* than in *pif3*.

Because this study systematically characterizes the role of PIF3-regulated genes in the dark, it was of interest to determine whether the *mida* mutants would be affected in the complete seedling etiolation development, and/or whether we would detect organ-specific actions. Based on the phenotypes of these four *mida* mutants, our data indicate that there is branching in the regulation of seedling deetiolation that PIF3 relays. Indeed, *MIDA9* and *MIDA10* are necessary for hook maintenance in the dark, whereas *MIDA11* regulates hypocotyl elongation, and *MIDA1* is involved in cotyledon separation (Figures 2, 3, and 4), indicating that these *MIDA* factors have organ-specific activity. One of these *MIDA* factors, *MIDA10*, is a negative regulator of hook unfolding (Figures 2 and 3). *MIDA10* encodes BBX23, a previously uncharacterized member of the *Arabidopsis* B-box family of transcription factors. Within this family, BBX23 forms part of a clade of eight members, four of which (BBX21, BBX22, BBX24, and BBX25) were previously implicated in light signaling (Khanna et al., 2006; Datta et al., 2007; Indorf et al., 2007) and possibly form a large complex with COP1 (Datta et al., 2008). BBX23 might also interact directly or indirectly with COP1. *MIDA9*, the second *MIDA* gene that participates in the regulation of hook maintenance as a negative regulator of hook unfolding, encodes a type 2C-phosphatase (PP2C) (Figures 2 and 3). Out of the 76 PP2Cs identified in *Arabidopsis* (Schweighofer et al., 2004), *MIDA9* is the only PP2C shown to be involved in seedling deetiolation. The third gene found to make a significant contribution to seedling deetiolation, specifically in the regulation of hypocotyl elongation, is *MIDA11* (Figures 2 and 4), a gene that encodes a MAP kinase. *MIDA11* has been recently reported to regulate auxin signaling in *Arabidopsis* roots (Lee et al., 2009). Interestingly, auxin participates in the induction of fast hypocotyl growth in dark-grown seedlings (De Grauwe et al., 2005). Also related to hormone signaling, the fourth gene, *MIDA1*, encodes HSD1, a hydroxysteroid dehydrogenase proposed to participate in the biosynthesis of BRs (Li et al., 2007). Adult *Arabidopsis* plants constitutively overexpressing HSD1 constitutively express BR response genes and display phenotypes similar to those of plants overproducing BR or the BR receptor, BRI1; that is, greater growth with increased branching and longer roots (Li et al., 2007). Based on the phenotype of BR-deficient mutants, BRs have also been shown to participate in seedling deetiolation (Li et al., 1996; Szekeres et al., 1996). Although more investigation is required, both *MIDA11* and *MIDA1* might contribute to the interplay between light and hormone signaling pathways, an integration that is essential for the coordination of seedling development (Halliday, 2004; Alabadi and Blázquez, 2009; Lau and Deng, 2010). Altogether, our data indicate that PIF3 signaling branches at a point where *MIDA9*, *MIDA10*, *MIDA11*, and *MIDA1* regulate different organ-specific pathways that might involve COP1 and hormone biosynthesis and/or signaling to coordinate the deetiolation response (see model in Figure 6D). Branching of the PIF3 signal might be achieved through differential spatial expression patterns of these *MIDA* factors in specific tissues or organs. More detailed analyses are required to assess this possibility (Bou-Torrent et al., 2008).

Eight out of the 12 tested loci seem not to have a significant role in regulating the hypocotyl, cotyledon, or hook responses downstream of PIF3 in the dark (Figure 2). Possible explanations for this lack of phenotype include: First, the expression changes detected in *pif3* for these *MIDA* genes might be functionally insignificant for the etiolated seedling, and thus irrelevant for the *pif3* phenotype in the dark. Although most of these genes are also targets of PIFq (see Supplemental Figures 4 and 6 online) and their expression is more robustly affected in *pifq*, correlating with the stronger phenotype, this remains a possibility. Second, some of these *MIDA* genes might cause a detectable phenotype when mutated, but this phenotype is not strong enough and/or sustained for long enough along dark development to meet our cutoff requirements for a bona fide phenotype and thus was not considered further (e.g., *mida11* and *mida12* in hook opening) (Figure 2; see Supplemental Data Set 5 online). Third, these genes might be relevant for PIF3-imposed seedling deetiolation, but functional redundancy with other factors ensures that disruption of a single gene does not have any phenotypic relevance. Functional redundancy is the most common explanation for lack of apparent phenotype, and the PIFs themselves exemplify this possibility (Leivar et al., 2008b; Shin et al., 2009). For the *MIDA* genes that lack an apparent phenotype, a search of the *Arabidopsis* databases reveals that two (*MIDA7* and *MIDA8*) belong to gene families (to the *CBL-INTERACTING PROTEIN KINASE* [*CIPK*] and the *HSD* gene families, respectively), and that *MIDA8* has another family member (*MIDA1*) that is also a PIF3 target (Gene Set 2) (Table 1). An assessment of possible functional redundancy in these cases would require the construction of higher-order combinations of the candidate genes. Finally, another possibility is that these *MIDA* factors might specifically affect deetiolation aspects that were not scored in our phenotypic analysis, such as chloroplast development or cotyledon expansion. More detailed analyses are needed to determine why mutation of each of these *MIDA* genes does not result in a dark seedling phenotype.

Given that PIF3 binds specifically to the G-box motif (Martínez-García et al., 2000; Shin et al., 2007), we inspected the 3-kb region upstream of the transcription start site of *MIDA* genes for the presence of the G-box motif CACGTG (See Methods) to determine whether functionally relevant *MIDAs* could potentially be directly regulated by PIF3. We found that of the four *MIDA* genes displaying a phenotype in the dark when mutated (*MIDA9*, *MIDA10*, *MIDA11*, and *MIDA1*) (Figures 3 and 4), only *MIDA9* had a G-box in its promoter sequence. Three other *MIDA* genes (*MIDA6*, *MIDA8*, and *MIDA13*) had G-boxes in their promoter sequences, but their mutants did not display a phenotype when examined in the dark (Figure 2), suggesting a lack of correlation in *MIDA* genes between the presence of a G-box in their promoters and the phenotypic effect in the dark when mutated.

### Light Regulation of PIF3 Signaling through the Organ-Specific *MIDA* Factors

Our data indicate that two of the *mida* mutants (*mida9* and *mida10*) exhibiting a similar phenotype in the dark (failure to maintain an apical hook) correspond to genes that are both negative regulators of hook opening and are regulated by PIF3 in

opposite directions in the dark: whereas *MIDA9* is repressed, *MIDA10* is induced by PIF3 (Figure 3, Table 1). This finding prompted us to hypothesize that this apparent contradiction might reflect the scenario played out once the wild-type etiolated seedling is exposed to light and PIF3 is degraded, rather than being a dark-specific phenomenon. A combination of Rc microarray data and detailed time courses analyzed by qRT-PCR (Figure 5; see Supplemental Figures 8 and 9 online) indicated that *MIDA10* is an early (1 h) light-repressed gene whose repression is maintained after 18 h of Rc, whereas *MIDA1* is early and transiently induced by light, and *MIDA9* and *MIDA11* show late light-induction after 3 to 6 h of Rc illumination (Figure 5; see Supplemental Figures 8 and 9 online). Our data show that these *MIDA* genes do not respond to light exposure simultaneously but rather in at least two temporally separated responses: one early (after 1 to 3 h of Rc) (*MIDA10* and *MIDA1*), and one late (after 3 to 6 h of Rc) (*MIDA9* and *MIDA11*). These data suggest that these *MIDA* factors that have a role in organ-specific seedling deetiolation might exert their function at different times, with those induced by light (*MIDA9*, *MIDA11*, and *MIDA1*) possibly extending their action beyond the dark period. Indeed, when we examined these *mida* mutants phenotypically in dark-to-red time courses, we detected that they also have defects in the deetiolation response upon Rc exposure (Figure 5B). Our data indicate that *MIDA11* is a negative regulator of hypocotyl elongation inhibition both in the dark and upon illumination, *MIDA1* is a positive regulator of cotyledon separation in the dark and during the first hours of red light illumination, and *MIDA10* is a negative regulator of hook opening in the dark and in the early initiation of deetiolation. Furthermore, *MIDA9* is a negative regulator of hook opening in the dark and during deetiolation, with a role that might be more prominent after 6 h of irradiation.

PIFs have been described as repressors of photomorphogenesis in the dark (Bae and Choi, 2008; Leivar et al., 2008b). The current model proposes that PIF action in the dark is exerted through the regulation of the expression of hundreds of genes by inducing presumptive repressors and by repressing presumptive inducers of photomorphogenesis, a function that is reversed by phy-induced PIF-degradation in response to light (Leivar et al., 2009; Shin et al., 2009). The functional profiling of PIF3-induced and -repressed genes presented here suggests an additional layer of complexity by which the PIF-phy system regulates deetiolation. Our data indicate that, in the dark, PIF3 both up- and downregulates inducers as well as repressors of photomorphogenesis, inducing the repressor *MIDA10* and the inducer *MIDA1*, and repressing the repressors *MIDA9* and *MIDA11* (see Supplemental Table 1 online). A model for the phy/PIF/*MIDA* mode of action is shown in Figures 6E and 6F. Given the partially deetiolated phenotype of *pif3*- in the dark, these findings suggest that the PIF system maintains a balance of inducer and repressor factors in the dark, with a preponderance of photomorphogenesis repressor activity, to maintain the etiolated state of the seedling in darkness. This action would be rapidly reversed upon light-induced degradation of the PIFs, shifting this balance to a dominance of photomorphogenesis inducer activity to initiate deetiolation. Accordingly, during this early and rapid initiation of seedling deetiolation (after 1 to 3 h of Rc), our data show that the repressor *MIDA10* is repressed in response to light, whereas the

inducer MIDA1 is induced by light. Furthermore, some of these MIDA regulators (MIDA9 and MIDA11) are late light-induced (after 3 to 6 h of Rc) (Figure 5A), suggesting that they act beyond the dark state and beyond the initial deetiolation trigger. Given that MIDA9 and MIDA11 correspond to repressors of photomorphogenesis (Figures 2, 3, and 5B) and that their induction takes place simultaneously with the late light repression of early inducers, such as MIDA1 (Figure 5A), our findings suggest that, after a few hours of illumination, once deetiolation is underway, the seedling again accumulates repressors of photomorphogenesis. These results are consistent with a scenario in which PIF3 regulates not only the rapid initial deetiolation trigger but also a subsequent counteractive response to prevent overresponses to light. In accordance, our data reveal that *pif3* and, to a greater extent, *pif3 pif4 pif5* are affected in the moderation of the initial light trigger and exhibit exaggerated cotyledon separation and inhibition of hypocotyl elongation, effects that are apparent after 1 to 2 d of Rc for cotyledon separation or after a few hours of illumination for hypocotyl response (Figures 6A to 6C). These data suggest that PIF3, together with other PIFs, such as PIF4 and PIF5, signal beyond the initial light trigger and exert a late repressive action to avoid excessive cotyledon separation and hypocotyl elongation inhibition. This late action is in apparent discrepancy with the rapid degradation of PIF3 in the light (Bauer et al., 2004; Monte et al., 2004; Park et al., 2004; Al-Sady et al., 2006). The late action of PIF3 could occur indirectly through secondary downstream targets and/or be exerted by the remaining light-stable pool of PIF3 (~10% of the levels in the dark) after the initial degradation (Monte et al., 2004). This late PIF-mediated process seems likely to be fundamental for seedling survival during the initial exposure to light. For example, it ensures that the cotyledons separate rapidly and are maintained at an angle parallel to the soil, optimal for light perception (Figures 6B and 6C). The existence of mechanisms that prevent overresponsiveness to the initial stimulus is an emerging theme in the regulation of responses to light, as has been described in the shade avoidance syndrome (Sessa et al., 2005) and, more recently, in responses to FR light (Li et al., 2010).

In conclusion, this study identifies downstream branching of PIF3 signaling as a means to optimize seedling deetiolation. We show that regulation of novel MIDA factors by the phy/PIF system enables the seedling to repress photomorphogenesis in the dark and respond optimally to light by regulating the abundance of positive and negative regulators of specific facets of photomorphogenesis, such as hypocotyl elongation, hook unfolding, and cotyledon separation. It will be of interest to determine how this regulation is achieved in the seedling by identifying additional PIF3-regulated components and the direct targets of PIF3 that orchestrate these organ-specific responses.

## METHODS

### Plant Material, Seedling Growth, and Measurements

T-DNA lines in the ecotype Col-0 background were identified by searching the Salk Institute Genomic Analysis Laboratory database (Alonso et al., 2003) (<http://signal.salk.edu/cgi-bin/tdnaexpress>). When possible, insertions within the promoter or in the 5'-region of the gene were favored

as specified in Table 1. Homozygous T-DNA insertion lines and wild-type siblings were identified using PCR with T-DNA- and gene-specific primers designed using the iSct Primers tool available in the Salk Institute Genomic Analysis Laboratory website. The primer sequences for each line can be found in Supplemental Table 2 online. For phenotypic analyses, two sibling mutant lines were compared with a wild-type sibling line and with the Col-0 controls. Wild-type and mutant seedlings were plated on GM medium without Suc as previously described (Monte et al., 2003). Seedlings were then stratified for 4 d at 4°C in darkness, induced to germinate with 3 h of WLC, and then placed in the dark for the indicated period of time. For hypocotyl, hook, and cotyledon measurements, seedlings grown for 2, 3, and 4 d were arranged horizontally on a plate and photographed using a digital camera (Nikon D80). Measurements were performed using NIH Image software (Image J, National Institutes of Health), as described before (Leivar et al., 2008b). Hook angle was measured as the angle between the hypocotyl and an imaginary line between the cotyledons, and cotyledon angle was measured as the angle between the central axes of the two cotyledons. Measurements of at least 30 seedlings for each mutant line were tested using Excel (Microsoft) for statistically significant differences with the wild-type sibling controls. P values were determined by Student's *t* test (equal variance, two-tailed distribution), and values below  $P = 0.05$  were considered statistically significant for differences in hypocotyl length, hook angle, or cotyledon angle between the wild-type and mutant lines. Mean values were used to calculate relative differences between the mutant and wild-type sibling, and phenotypes were expressed relative to the wild-type sibling value set at unity. Representative lines for each mutant were used in Figure 2 and Supplemental Data Set 5 online, whereas Figures 3 and 4 show all lines used in the analysis of the selected genes. For the red light treatments shown in Figure 5, seedlings were transferred after dark growth to Rc (8  $\mu\text{mol}/\text{m}^2/\text{s}$ ) for the time indicated. For the cotyledon separation experiment shown in Figure 6, cotyledon angle was calculated as specified above except for angles exceeding 180°, where outer angles were measured and corrections applied, because Image J only measures angles between 0° and 180°. For the FR treatments shown in Supplemental Figure 10 online, seedlings were transferred after 21 h of dark growth to continuous FR (0.01  $\mu\text{mol}/\text{m}^2/\text{s}$ ) at 21°C for 3 d. Control seedlings were kept in darkness. The DEX treatment shown in Figure 4 was performed using DEX (Sigma-Aldrich) diluted in HPLC-grade ethanol (minimum 98%) at a concentration of 5  $\mu\text{M}$ .

### Microarray-Based Expression Profiling: Samples and Data Analysis

Samples for microarray experiments in the dark correspond to samples in Monte et al. (2004), with the exception of R18 h and D18 h, which were part of the same experiment but were not included in the original analysis. Briefly, three biological replicates of wild-type and *pif3-3* seedlings were grown separately in GM medium without Suc for 4 d (96 h) in the dark (D0 h time point) as previously described (Monte et al., 2003). For dark treatments, D0 h (D96 h) and D1 h (D97 h) samples were harvested 1 h apart and were used in this work to identify PIF3-regulated genes in the dark. For red light treatments, 4-d-old wild-type seedlings were transferred to Rc (8  $\mu\text{mol}/\text{m}^2/\text{s}$ ) at D0 h, and samples were collected after 1 h (R1 h) and 18 h (R18 h), together with controls at D1 h and D18 h. These red light-treated samples and their dark controls were used in this work to identify early (R1 h) and late (R18 h) red light-responsive genes.

Dark data analysis was performed using the Rosetta Resolver Gene Expression Analysis System, version 7.0 (Rosetta Biosoftware). A gene list of transcripts whose expression is significantly altered by the *PIF3* mutation in 4-d-old, dark-grown seedlings was calculated by performing a two-group, two-way, error-weighted, Benjamini-Hochberg false discovery rate error-corrected analysis of variance comparing D0 h and D1 h samples for the wild type and *pif3*, with a *P*-value cutoff of 0.05, resulting

in 1402 significant transcripts. This statistical significance test was combined with experimental consistency by further reducing the statistically significant transcript list to only those transcripts exhibiting an absolute FC of greater than 1.5-fold in both D0 h and D1 h conditions. This resulted in a nonredundant list of 122 transcripts (statistically and significantly different by an absolute FC of 1.5, SS1.5F). Next, a ratio error model (Weng et al., 2006) that reduced the transcript list to 82 HC PIF3 target genes in the dark (SS1.5F-HC) was applied.

To identify early and late red light-responsive genes, wild-type red (R1 h and R18 h) and wild-type dark samples (D1 h and D18 h) were analyzed at each time point using the Rosetta Resolver Gene Expression Analysis System, version 7.0 (Rosetta Biosoftware). A list of Rc-responsive transcripts was calculated by performing a ratio analysis applying a ratio error model cutoff of 0.05 (Weng et al., 2006) and an absolute FC of greater than twofold. These analyses resulted in 546 significant transcripts (statistically and significantly different by an absolute FC of 2; SS2F) for R1 h, and 2764 SS2F genes for R18 h.

### Gene Expression Analysis

For the RNA gel blot analyses in Figure 3, total RNA was isolated from 2-d-old, dark-grown seedlings using the RNeasy Plant Mini Kit (Qiagen), according to a previously described procedure (Monte et al., 2003). Gene-specific probes were amplified by PCR and labeled by random priming (Roche). Primer sequences can be found in Supplemental Table 2 online. Hybridization signal was detected with a Storm 860 Phosphor-Imager (Molecular Dynamics).

For qRT-PCR analysis, seedlings were grown in the dark for the indicated times (for Figure 4; see Supplemental Figures 2 and 6 online) or subsequently treated with red light ( $8 \mu\text{mol}/\text{m}^2/\text{s}$ ) for up to 12 h for the analysis shown in Figure 5B. qRT-PCR analysis was performed as described previously (Khanna et al., 2007) with variations. Briefly,  $10 \mu\text{g}$  of total RNA extracted using the RNeasy Plant Mini Kit (Qiagen) were treated with DNase (Ambion) according to the manufacturer's instructions. First-strand cDNA synthesis was performed using the SuperScript III reverse transcriptase (Invitrogen) and oligo dT as a primer (dT30). cDNA was then treated with RNase Out (Invitrogen) before 1:20 dilution with water, and  $20 \mu\text{L}$  was used for real-time PCR (Light Cycler 480; Roche) using SYBR Premix Ex Taq (Takara) and primers at a 300 nM concentration. Each PCR was repeated at least two times, and the mean expression values from these technical replicates were used for further calculations. Gene expression was measured from at least two biological replicates, and *PP2A* was used as a normalization control as described previously (Shin et al., 2007). Normalized gene expression is represented relative to the dark-grown wild-type set at unity. Primer sequences for qRT-PCR can be found in Supplemental Table 2 online.

### Promoter Analysis for Presence of G-Box Motifs

Promoter analysis was performed using the "Motif Analysis" tool available at The Arabidopsis Information Resource (<http://Arabidopsis.org/tools/bulk/motiffinder/index.jsp>) to look for the CACGTG G-box motif in the 3-kb region upstream of the start codon of each of the *MIDA* genes.

### Accession Numbers

The microarray data reported in this publication have been deposited in the National Center for Biotechnology Information Gene Expression Omnibus (GEO; <http://www.ncbi.nlm.nih.gov/geo/>) under the GEO Series accession number GSE30030. Sequence data can be found in the *Arabidopsis* Genome Initiative database under accession numbers AT5G50600 (*MIDA1/HSD1*), AT3G05730 (*MIDA2*), AT4G37300 (*MIDA3*), AT1G02470 (*MIDA4*), AT3G47250 (*MIDA5*), AT5G04340 (*MIDA6*), AT1G48260 (*MIDA7/CIPK17*), AT4G10020 (*MIDA8/HSD5*), AT5G02760

(*MIDA9*), AT4G10240 (*MIDA10/BBX23*), AT2G46070 (*MIDA11/MPK12*), AT1G05510 (*MIDA12*), AT5G45690 (*MIDA13*), and *PP2A* (AT1G13320).

### Supplemental Data

The following materials are available in the online version of this article.

**Supplemental Figure 1.** PIF3 Regulation of Gene Expression in the Dark.

**Supplemental Figure 2.** Distribution of PIF3-Regulated Genes among Functional Categories.

**Supplemental Figure 3.** qRT-PCR Validation of Microarray Data.

**Supplemental Figure 4.** Comparative Expression Analysis of PIF3 Function with Other PIF Factors in the Dark.

**Supplemental Figure 5.** Comparison of *pif3*-D SSTF-HC Genes versus *pifq*-D and *pif4pif5*-D.

**Supplemental Figure 6.** Expression of *MIDA* Genes in *pif3* and *pifq*.

**Supplemental Figure 7.** Characterization of *mida9-2*.

**Supplemental Figure 8.** Light-Responsiveness of PIF3-Regulated Genes in the Dark.

**Supplemental Figure 9.** Microarray Data Displaying the Mean Expression Level of *MIDA10*, *MIDA9*, *MIDA11*, and *MIDA1* after 1 h and 18 h of Rc Treatment.

**Supplemental Figure 10.** Hook Angle Phenotype Displayed by *mida9-1* in Continuous FR.

**Supplemental Figure 11.** Quantification of Hypocotyl Length Displayed by *mida11* in the Dark-to-Light Transition in the Absence of DEX.

**Supplemental Figure 12.** Quantification of Hypocotyl Length in *pif3* and Cotyledon Separation Angle in *pif3* and *pif3 pif4 pif5* after Dark-to-Light Transition.

**Supplemental Table 1.** Summary of *MIDA9*, *MIDA10*, *MIDA11*, and *MIDA1* Gene Regulation by PIF3 and by Red Light, as well as the Phenotype of Their Respective *Arabidopsis* Mutants.

**Supplemental Table 2.** Primer Sequences Used for PCR Amplification.

**Supplemental Analysis 1.** Definition of the PIF3-Regulated Transcriptome in the Dark.

**Supplemental Analysis 2.** Functional Classification of PIF3-Regulated Genes in the Dark.

**Supplemental Analysis 3.** Comparative Analysis of PIF3-, PIF4PIF5-, and PIFq-regulated Transcriptomes in the Dark.

**Supplemental Analysis 4.** Comparative Analysis of PIF3-Regulated Transcriptome in the Dark with Genes Displaying SSTF Alterations in the Wild Type after 1 h and 18 h of Red Light Treatment.

**Supplemental References 1.** The Supplemental References for Supplemental Analyses 1 to 4.

**Supplemental Data Set 1.** Expression Data and Statistical Analysis for the SS1.5F Genes at D0 h and D1 h Reported in Figure 1 and Supplemental Figure 1 online.

**Supplemental Data Set 2.** Expression Data and Statistical Analysis for the SS1.5F-HC Genes at D0 h and D1 h Reported in Figure 1 and Supplemental Figure 1 online.

**Supplemental Data Set 3.** List of SS1.5F Genes That Do Not Meet the Requirements to be Designated as SS1.5F-HC Genes as Reported in Supplemental Figure 1 online.



**Supplemental Data Set 4.** List of Class P3, P3/PQ, P3/P4P5, and P4P5/PQ Genes Reported in Supplemental Figure 4 online.

**Supplemental Data Set 5.** Primary Data and Statistical Analysis for *mida* Mutant Phenotypic Characterization Shown in Figure 2.

**Supplemental Data Set 6.** List of Early Light-Responsive Genes in Dark-Grown Wild-Type Seedlings after 1 h of Red Light Treatment (8  $\mu\text{mol}/\text{m}^2/\text{s}$ ) Reported in Supplemental Figure 8 online.

**Supplemental Data Set 7.** List of Late Light-Responsive Genes in Dark-Grown Wild-Type Seedlings after 18 h of Red Light Treatment (8  $\mu\text{mol}/\text{m}^2/\text{s}$ ) Reported in Supplemental Figure 8 online.

**Supplemental Data Set 8.** List of Induced Class 1 to 3 Genes (Ind-Class) and Repressed Class 1 to 4 Genes (Rep-Class) as Defined in Supplemental Figure 8 online.

## ACKNOWLEDGMENTS

We thank Adrian J. Cutler for AOHSD seeds (*mida1-OX*) (Li et al., 2007) and Brian E. Ellis for MPK12RNAi seeds (*mida11*) (Lee et al., 2009). SALK (Alonso et al., 2003) and SAIL T-DNA lines were obtained from Nottingham Arabidopsis Stock Centre. We thank Josep M. Casacuberta for helpful comments on the manuscript. This work was supported by a Junta para la Ampliación de Estudios predoctoral fellowship from Consejo Superior de Investigaciones Científicas to J.S. (JaePre\_08\_01049), by a “Comissionat per a Universitats i Recerca del Departament d’Innovació, Universitats i Empresa” fellowship of the Generalitat de Catalunya (Beatriu de Pinós program) and Marie Curie IRG PIRG06-GA-2009-256420 grant to P.L., and by Marie Curie IRG-046568, Spanish “Ministerio de Ciencia e Innovación” BIO2006-09254 and BIO2009-07675, and Generalitat de Catalunya 2009-SGR-206 grants to E.M.

## AUTHOR CONTRIBUTIONS

M.S., P.L., P.Q., and E.M. designed the research; M.S., G.M., N.G., J.S., J.T., and E.M. performed research. M.S. and E.M. analyzed data; and M.S., P.L., P.Q., and E.M. wrote the article.

Received June 19, 2011; revised September 7, 2011; accepted November 3, 2011; published November 22, 2011.

## REFERENCES

- Alabádi, D., and Blázquez, M.A. (2009). Molecular interactions between light and hormone signaling to control plant growth. *Plant Mol. Biol.* **69**: 409–417.
- Alonso, J.M., et al. (2003). Genome-wide insertional mutagenesis of *Arabidopsis thaliana*. *Science* **301**: 653–657.
- Al-Sady, B., Ni, W., Kircher, S., Schäfer, E., and Quail, P.H. (2006). Photoactivated phytochrome induces rapid PIF3 phosphorylation prior to proteasome-mediated degradation. *Mol. Cell* **23**: 439–446.
- Bae, G., and Choi, G. (2008). Decoding of light signals by plant phytochromes and their interacting proteins. *Annu. Rev. Plant Biol.* **59**: 281–311.
- Bauer, D., Viczián, A., Kircher, S., Nobis, T., Nitschke, R., Kunkel, T., Panigrahi, K.C.S., Adám, E., Fejes, E., Schäfer, E., and Nagy, F. (2004). Constitutive photomorphogenesis 1 and multiple photoreceptors control degradation of phytochrome interacting factor 3, a transcription factor required for light signaling in *Arabidopsis*. *Plant Cell* **16**: 1433–1445.
- Bou-Torrent, J., Roig-Villanova, I., and Martínez-García, J.F. (2008). Light signaling: Back to space. *Trends Plant Sci.* **13**: 108–114.
- Castillon, A., Shen, H., and Huq, E. (2007). Phytochrome Interacting Factors: Central players in phytochrome-mediated light signaling networks. *Trends Plant Sci.* **12**: 514–521.
- Datta, S., Hettiarachchi, C., Johansson, H., and Holm, M. (2007). SALT TOLERANCE HOMOLOG2, a B-box protein in *Arabidopsis* that activates transcription and positively regulates light-mediated development. *Plant Cell* **19**: 3242–3255.
- Datta, S., Johansson, H., Hettiarachchi, C., Irigoyen, M.L., Desai, M., Rubio, V., and Holm, M. (2008). LZFI/SALT TOLERANCE HOMOLOG3, an *Arabidopsis* B-box protein involved in light-dependent development and gene expression, undergoes COP1-mediated ubiquitination. *Plant Cell* **20**: 2324–2338.
- De Grauwe, L., Vandebussche, F., Tietz, O., Palme, K., and Van Der Straeten, D. (2005). Auxin, ethylene and brassinosteroids: Tripartite control of growth in the *Arabidopsis* hypocotyl. *Plant Cell Physiol.* **46**: 827–836.
- de Lucas, M., Davière, J.M., Rodríguez-Falcón, M., Pontin, M., Iglesias-Pedraz, J.M., Lorrain, S., Fankhauser, C., Blázquez, M.A., Titarenko, E., and Prat, S. (2008). A molecular framework for light and gibberellin control of cell elongation. *Nature* **451**: 480–484.
- Duek, P.D., and Fankhauser, C. (2005). bHLH class transcription factors take centre stage in phytochrome signalling. *Trends Plant Sci.* **10**: 51–54.
- Fujimori, T., Yamashino, T., Kato, T., and Mizuno, T. (2004). Circadian-controlled basic/helix-loop-helix factor, PIL6, implicated in light-signal transduction in *Arabidopsis thaliana*. *Plant Cell Physiol.* **45**: 10781086.
- Halliday, K.J. (2004). Plant hormones: The interplay of brassinosteroids and auxin. *Curr. Biol.* **14**: R1008–R1010.
- Huq, E., and Quail, P.H. (2002). PIF4, a phytochrome-interacting bHLH factor, functions as a negative regulator of phytochrome B signaling in *Arabidopsis*. *EMBO J.* **21**: 2441–2450.
- Huq, E., Al-Sady, B., Hudson, M., Kim, C., Apel, K., and Quail, P.H. (2004). Phytochrome-interacting factor 1 is a critical bHLH regulator of chlorophyll biosynthesis. *Science* **305**: 1937–1941.
- Indorf, M., Cordero, J., Neuhaus, G., and Rodríguez-Franco, M. (2007). Salt tolerance (STO), a stress-related protein, has a major role in light signalling. *Plant J.* **51**: 563–574.
- Jang, I.C., Henriques, R., Seo, H.S., Nagatani, A., and Chua, N.H. (2010). *Arabidopsis* PHYTOCHROME INTERACTING FACTOR proteins promote phytochrome B polyubiquitination by COP1 E3 ligase in the nucleus. *Plant Cell* **22**: 2370–2383.
- Jiao, Y., Lau, O.S., and Deng, X.W. (2007). Light-regulated transcriptional networks in higher plants. *Nat. Rev. Genet.* **8**: 217–230.
- Josse, E.M., and Halliday, K.J. (2008). Skotomorphogenesis: The dark side of light signalling. *Curr. Biol.* **18**: R1144–R1146.
- Khanna, R., Kronmiller, B., Maszle, D.R., Coupland, G., Holm, M., Mizuno, T., and Wu, S.H. (2009). The *Arabidopsis* B-box zinc finger family. *Plant Cell* **21**: 3416–3420.
- Khanna, R., Shen, Y., Marion, C.M., Tsuchisaka, A., Theologis, A., Schäfer, E., and Quail, P.H. (2007). The basic helix-loop-helix transcription factor PIF5 acts on ethylene biosynthesis and phytochrome signaling by distinct mechanisms. *Plant Cell* **19**: 3915–3929.
- Khanna, R., Shen, Y., Toledo-Ortiz, G., Kikis, E.A., Johannesson, H., Hwang, Y.S., and Quail, P.H. (2006). Functional profiling reveals that only a small number of phytochrome-regulated early-response genes in *Arabidopsis* are necessary for optimal deetiolation. *Plant Cell* **18**: 2157–2171.
- Kim, J.Y., Yi, H.K., Choi, G., Shin, B., Song, P.S., and Choi, G.S. (2003). Functional characterization of phytochrome interacting factor 3 in phytochrome-mediated light signal transduction. *Plant Cell* **15**: 2399–2407.
- Lau, O.S., and Deng, X.W. (2010). Plant hormone signaling lightens up: Integrators of light and hormones. *Curr. Opin. Plant Biol.* **13**: 571–577.
- Lee, J.S., Wang, S., Sritubtim, S., Chen, J.G., and Ellis, B.E. (2009). *Arabidopsis* mitogen-activated protein kinase MPK12 interacts with

- the MAPK phosphatase IBR5 and regulates auxin signaling. *Plant J.* **57**: 975–985.
- Leivar, P., and Quail, P.H.** (2011). PIFs: Pivotal components in a cellular signaling hub. *Trends Plant Sci.* **16**: 19–28.
- Leivar, P., Tepperman, J.M., Monte, E., Calderon, R.H., Liu, T.L., and Quail, P.H.** (2009). Definition of early transcriptional circuitry involved in light-induced reversal of PIF-imposed repression of photomorphogenesis in young *Arabidopsis* seedlings. *Plant Cell* **21**: 3535–3553.
- Leivar, P., Monte, E., Al-Sady, B., Carle, C., Storer, A., Alonso, J.M., Ecker, J.R., and Quail, P.H.** (2008a). The *Arabidopsis* phytochrome-interacting factor PIF7, together with PIF3 and PIF4, regulates responses to prolonged red light by modulating phyB levels. *Plant Cell* **20**: 337–352.
- Leivar, P., Monte, E., Oka, Y., Liu, T., Carle, C., Castillon, A., Huq, E., and Quail, P.H.** (2008b). Multiple phytochrome-interacting bHLH transcription factors repress premature seedling photomorphogenesis in darkness. *Curr. Biol.* **18**: 1815–1823.
- Li, F., Asami, T., Wu, X., Tsang, E.W., and Cutler, A.J.** (2007). A putative hydroxysteroid dehydrogenase involved in regulating plant growth and development. *Plant Physiol.* **145**: 87–97.
- Li, J., Nagpal, P., Vitart, V., McMorris, T.C., and Chory, J.** (1996). A role for brassinosteroids in light-dependent development of *Arabidopsis*. *Science* **272**: 398–401.
- Li, J., Li, G., Gao, S., Martinez, C., He, G., Zhou, Z., Huang, X., Lee, J.H., Zhang, H., Shen, Y., Wang, H., and Deng, X.W.** (2010). *Arabidopsis* transcription factor ELONGATED HYPOCOTYL5 plays a role in the feedback regulation of phytochrome A signaling. *Plant Cell* **22**: 3634–3649.
- Lorrain, S., Trevisan, M., Pradervand, S., and Fankhauser, C.** (2009). Phytochrome interacting factors 4 and 5 redundantly limit seedling de-etiolation in continuous far-red light. *Plant J.* **60**: 449–461.
- Lorrain, S., Allen, T., Duek, P.D., Whitelam, G.C., and Fankhauser, C.** (2008). Phytochrome-mediated inhibition of shade avoidance involves degradation of growth-promoting bHLH transcription factors. *Plant J.* **53**: 312–323.
- Martínez-García, J.F., Huq, E., and Quail, P.H.** (2000). Direct targeting of light signals to a promoter element-bound transcription factor. *Science* **288**: 859–863.
- Monte, E., Al-Sady, B., Leivar, P., and Quail, P.H.** (2007). Out of the dark: How the PIFs are unmasking a dual temporal mechanism of phytochrome signalling. *J. Exp. Bot.* **58**: 3125–3133.
- Monte, E., Alonso, J.M., Ecker, J.R., Zhang, Y., Li, X., Young, J., Austin-Phillips, S., and Quail, P.H.** (2003). Isolation and characterization of phyC mutants in *Arabidopsis* reveals complex crosstalk between phytochrome signaling pathways. *Plant Cell* **15**: 1962–1980.
- Monte, E., Tepperman, J.M., Al-Sady, B., Kaczorowski, K.A., Alonso, J.M., Ecker, J.R., Li, X., Zhang, Y.L., and Quail, P.H.** (2004). The phytochrome-interacting transcription factor, PIF3, acts early, selectively, and positively in light-induced chloroplast development. *Proc. Natl. Acad. Sci. USA* **101**: 16091–16098.
- Moon, J., Zhu, L., Shen, H., and Huq, E.** (2008). PIF1 directly and indirectly regulates chlorophyll biosynthesis to optimize the greening process in *Arabidopsis*. *Proc. Natl. Acad. Sci. USA* **105**: 9433–9438.
- Nagatani, A.** (2004). Light-regulated nuclear localization of phytochromes. *Curr. Opin. Plant Biol.* **7**: 708–711.
- Nozue, K., Covington, M.F., Duek, P.D., Lorrain, S., Fankhauser, C., Harmer, S.L., and Maloof, J.N.** (2007). Rhythmic growth explained by coincidence between internal and external cues. *Nature* **448**: 358–361.
- Oh, E., Yamaguchi, S., Kamiya, Y., Bae, G., Chung, W.I., and Choi, G.** (2006). Light activates the degradation of PIL5 protein to promote seed germination through gibberellin in *Arabidopsis*. *Plant J.* **47**: 124–139.
- Parks, B.M., and Spalding, E.P.** (1999). Sequential and coordinated action of phytochromes A and B during *Arabidopsis* stem growth revealed by kinetic analysis. *Proc. Natl. Acad. Sci. USA* **96**: 14142–14146.
- Park, E., Kim, J., Lee, Y., Shin, J., Oh, E., Chung, W.I., Liu, J.R., and Choi, G.** (2004). Degradation of phytochrome interacting factor 3 in phytochrome-mediated light signaling. *Plant Cell Physiol.* **45**: 968–975.
- Quail, P.H.** (2002). Phytochrome photosensory signalling networks. *Nat. Rev. Mol. Cell Biol.* **3**: 85–93.
- Quail, P.H.** (2010). Phytochromes. *Curr. Biol.* **20**: R504–R507.
- Rockwell, N.C., Su, Y.S., and Lagarias, J.C.** (2006). Phytochrome structure and signaling mechanisms. *Annu. Rev. Plant Biol.* **57**: 837–858.
- Schäfer, E., and Nagy, F.** (2006). Photomorphogenesis in Plants and Bacteria. (Dordrecht, The Netherlands: Springer).
- Schweighofer, A., Hirt, H., and Meskiene, I.** (2004). Plant PP2C phosphatases: Emerging functions in stress signaling. *Trends Plant Sci.* **9**: 236–243.
- Sessa, G., Carabelli, M., Sassi, M., Ciolfi, A., Possenti, M., Mitterpergher, F., Becker, J., Morelli, G., and Ruberti, I.** (2005). A dynamic balance between gene activation and repression regulates the shade avoidance response in *Arabidopsis*. *Genes Dev.* **19**: 2811–2815.
- Shen, H., Moon, J., and Huq, E.** (2005). PIF1 is regulated by light-mediated degradation through the ubiquitin-26S proteasome pathway to optimize photomorphogenesis of seedlings in *Arabidopsis*. *Plant J.* **44**: 1023–1035.
- Shen, Y., Khanna, R., Carle, C.M., and Quail, P.H.** (2007). Phytochrome induces rapid PIF5 phosphorylation and degradation in response to red-light activation. *Plant Physiol.* **145**: 1043–1051.
- Shen, H., Zhu, L., Castillon, A., Majee, M., Downie, B., and Huq, E.** (2008). Light-induced phosphorylation and degradation of the negative regulator PHYTOCHROME-INTERACTING FACTOR1 from *Arabidopsis* depend upon its direct physical interactions with photoactivated phytochromes. *Plant Cell* **20**: 1586–1602.
- Shin, J., Park, E., and Choi, G.** (2007). PIF3 regulates anthocyanin biosynthesis in an HY5-dependent manner with both factors directly binding anthocyanin biosynthetic gene promoters in *Arabidopsis*. *Plant J.* **49**: 981–994.
- Shin, J., Kim, K., Kang, H., Zulfugarov, I.S., Bae, G., Lee, C.H., Lee, D., and Choi, G.** (2009). Phytochromes promote seedling light responses by inhibiting four negatively-acting phytochrome-interacting factors. *Proc. Natl. Acad. Sci. USA* **106**: 7660–7665.
- Stephenson, P.G., Fankhauser, C., and Terry, M.J.** (2009). PIF3 is a repressor of chloroplast development. *Proc. Natl. Acad. Sci. USA* **106**: 7654–7659.
- Szekeres, M., Németh, K., Koncz-Kálmán, Z., Mathur, J., Kauschmann, A., Altmann, T., Rédei, G.P., Nagy, F., Schell, J., and Koncz, C.** (1996). Brassinosteroids rescue the deficiency of CYP90, a cytochrome P450, controlling cell elongation and de-etiolation in *Arabidopsis*. *Cell* **85**: 171–182.
- Toledo-Ortiz, G., Huq, E., and Quail, P.H.** (2003). The *Arabidopsis* basic/helix-loop-helix transcription factor family. *Plant Cell* **15**: 1749–1770.
- Toledo-Ortiz, G., Huq, E., and Rodríguez-Concepción, M.** (2010). Direct regulation of phytoene synthase gene expression and carotenoid biosynthesis by phytochrome-interacting factors. *Proc. Natl. Acad. Sci. USA* **107**: 11626–11631.
- Weng, L., Dai, H., Zhan, Y., He, Y., Stepaniants, S.B., and Bassett, D.E.** (2006). Rosetta error model for gene expression analysis. *Bioinformatics* **22**: 1111–1121.
- Yamaguchi, R., Nakamura, M., Mochizuki, N., Kay, S.A., and Nagatani, A.** (1999). Light-dependent translocation of a phytochrome B-GFP fusion protein to the nucleus in transgenic *Arabidopsis*. *J. Cell Biol.* **145**: 437–445.